
Reverse Diffusion Sequential Monte Carlo Samplers

Luhuan Wu*

Columbia University

Yi Han

Columbia University

Christian A. Naesseth

University of Amsterdam

John P. Cunningham

Columbia University

Abstract

We propose a novel sequential Monte Carlo (SMC) method for sampling from unnormalized target distributions based on a reverse denoising diffusion process. While recent diffusion-based samplers simulate the reverse diffusion using approximate score functions, they can suffer from accumulating errors due to time discretization and imperfect score estimation. In this work, we introduce a principled SMC framework that formalizes diffusion-based samplers as proposals while systematically correcting for their biases. The core idea is to construct informative intermediate target distributions that progressively steer the sampling trajectory toward the final target distribution. Although ideal intermediate targets are intractable, we develop *exact* approximations using quantities from the score estimation-based proposal, without requiring additional model training or inference overhead. The resulting sampler, termed *Reverse Diffusion Sequential Monte Carlo*, enables consistent sampling and unbiased estimation of the target’s normalization constant under mild conditions. We demonstrate the effectiveness of our method on a range of synthetic targets and real-world Bayesian inference problems.

1 Introduction

Sampling from unnormalized target distributions is a fundamental problem in many applications, ranging from Bayesian inference [1, 2] to simulating molecular systems [3]. Classical methods like Markov chain Monte Carlo (MCMC) simulate a Markov chain with the target as its stationary distribution, but they can suffer from slow mixing and difficulty traversing between modes for complex distributions. Particle-based methods, such as importance sampling, generate exact samples in a large compute limit; yet they struggle with the curse of dimensionality [4]. Alternatively, variational inference (VI) [5] reframes inference as an optimization task, though its success depends on the expressiveness of the variational family and the complexity of the optimization landscape.

Recently, diffusion models have gained traction as a powerful class of generative models for sampling from complex distributions. Diffusion models construct a forward noising process that gradually transforms a complex target distribution into a simple reference distribution [6, 7]. A reverse denoising process is then used to recover target samples from the reference, guided by a time-dependent score function. In the generative modeling setting, this score function is approximated by a neural network trained on samples from the target distribution.

In the sampling context, where such training data is unavailable, recent works have extended the diffusion paradigm by leveraging information from the unnormalized target density. Huang et al. [8], Grenioux et al. [9] estimate the score function using MCMC samples from denoising posteriors of the target, and then simulate from a discretized reverse diffusion process guided by these estimates.

*Correspondence email: 1w2827@columbia.edu

This approach demonstrates both theoretical and empirical advantages over conventional Langevin-style MCMC methods, particularly for multi-modal distributions.

A parallel line of research explores diffusion-based neural samplers, which train a neural network to approximate the score function using only the target information. Phillips et al. [10], Akhoud-Sadegh et al. [11], Ou Yang et al. [12] use novel score matching losses, while VI-based methods [13, 14, 15, 16, 17] learn the score by optimizing a divergence between forward and reverse processes.

While promising, diffusion-based sampling methods suffer from two sources of bias: discretization error in simulating the reverse diffusion dynamics and approximation error in the estimated or learned score function. Exceptions are Phillips et al. [10] and Chen et al. [18], which reduce the bias of diffusion-based neural samplers using Sequential Monte Carlo (SMC) – a general tool for sequential inference [19]. However, a recent survey finds that neural samplers still fall short in training efficiency and often rely on special network preconditioning, compared to classical sampling methods [20].

To address these challenges, we develop a training-free diffusion-based sampler, *Reverse Diffusion Sequential Monte Carlo* (RDSMC), which offers theoretical guarantees. Inspired by previous work, we formalize the diffusion-based sampler as a proposal mechanism within an SMC framework. At a high level, our algorithm generates multiple trajectories, or *particles*, from the reverse diffusion process using estimated scores. To correct for estimation and discretization biases, we design intermediate target distributions to guide resampling of particles at each step, progressively steering them toward the final target distribution of interest.

Crucially, our intermediate target distributions are constructed from byproducts of score estimation, without additional training or computational overhead. These targets align with the marginal distributions induced by the final target and the forward noising process, resulting in an *exact approximation* [21, 22]. In contrast, Phillips et al. [10] learn neural network-based alternatives which only attain the true marginal at the final step, and Chen et al. [18] prescribe an annealing path to guide the particles.

RDSMC belongs to a class of nested SMC methods [23], inheriting the standard SMC guarantees. In particular, it produces asymptotically exact samples from the target in the limit of many particles, and provides an unbiased estimate of the normalization constant for any fixed size of particles.

Our contributions are summarized as follows:

- We propose a new SMC algorithm, Reverse Diffusion Sequential Monte Carlo (RDSMC), based on the diffusion paradigm for sampling from an unnormalized distribution.
- RDSMC is training-free, provides an unbiased estimate of the normalization constant, and is asymptotically exact.
- We show through experiments that RDSMC outperforms or matches existing diffusion-based samplers and classical geometric annealing-based Annealed Importance Sampling [AIS, 24] and SMC samplers [25] on synthetic targets and Bayesian logistic regression benchmarks.

2 Background

Diffusion models. Diffusion models [6, 7] evolve a complex target distribution $\pi(x)$ into a simple reference distribution $p_1(x)$, via a forward stochastic differential equation (SDE)

$$dx(\tau) = f(\tau)x(\tau)d\tau + g(\tau)dB_\tau, \quad \tau \in [0, 1], \quad (1)$$

where $f(\tau)$ and $g(\tau)$ are the drift and diffusion coefficients, and B_τ is standard Brownian motion.

To generate samples from $\pi(x)$, we simulate a reverse SDE initialized from $x(1) \sim p_1(x)$,

$$dx(\tau) = [f(\tau)x(\tau) - g(\tau)^2 \nabla_x \log p_\tau(x)|_{x=x(\tau)}] d\tau + g(\tau)d\bar{B}_\tau, \quad \tau \in [1, 0], \quad (2)$$

where $\nabla_x \log p_\tau(x)$ is the score function of the marginal density $p_\tau(x)$ at time τ , and \bar{B}_τ is the reverse-time Brownian motion.

While the score function is typically intractable, it can be approximated by training a score network on samples from the target $\pi(x)$. Once trained, the score network is substituted into the reverse SDE, which is then discretized to generate samples from $\pi(x)$.

Diffusion-based samplers. In the sampling setting, we are given access to the unnormalized density of $\pi(x)$ rather than its samples. In this case, score estimation can be translated into a posterior inference problem. For example, the denoising score identity [DSI, 26], or Tweedie’s formula [27], provides an expression for the score function,

$$\nabla_x \log p_\tau(x) = \int \frac{\alpha(\tau)x_0 - x}{\sigma(\tau)^2} p_\tau(x_0 | x) dx_0, \quad (3)$$

where $p_\tau(x_0 | x) \propto \pi(x_0) \mathcal{N}(x | \alpha(\tau)x_0, \sigma(\tau)^2 \mathbb{I})$ is the posterior with the target as prior and the forward kernel as the likelihood parameterized by $\alpha(\tau)$ and $\sigma(\tau)$ (see Appendix A.1 for expressions).

Huang et al. [8], Grenioux et al. [9] estimate the score using DSI via MCMC samples from $p_\tau(x_0 | x)$, which is then used to simulate the reverse diffusion process in Eq. (2), starting from a Langevin-style initialization. See § 4 for further discussion of related approaches.

Sequential Monte Carlo. Sequential Monte Carlo (SMC) is a particle-based method for approximately sampling from a sequence of distributions defined on variables $x_{0:T}$, terminating at a final distribution of interest. We consider a reverse-time formulation, where SMC evolves a weighted collection of N particles $\{x_t^{(i)}, w_t^{(i)}\}_{i=1}^N$ from $t = T$ to 0, gradually approximating the final target.

An SMC sampler requires two key design choices [22], a sequence of intermediate proposals, $q(x_T)$ and $\{q(x_t | x_{t+1})\}_{t=0}^{T-1}$, and a sequence of (unnormalized) intermediate target distributions, $\{\gamma_t(x_{t:T})\}_{t=0}^T$, such that the final target $\gamma_0(x_{0:T})$ recovers the distribution of interest.

The procedure initializes with N particles $x_T^{(i)} \sim q_T(x_T)$ and weights $w_T^{(i)} \leftarrow \gamma_T(x_T^{(i)}) / q(x_T^{(i)})$ for $i = 1, \dots, N$. Then for each step $t = T-1, \dots, 0$ and particle $i = 1, \dots, N$, SMC proceeds as follows: (1) resample ancestor $x_{t+1}^{(i)} \sim \text{Multinomial}(x_{t+1}^{(1:N)}, w_{t+1}^{(1:N)})$; (2) propagate particle $x_t^{(i)} \sim q(x_t | x_{t+1}^{(i)})$; (3) compute weight $w_t^{(i)} \leftarrow \gamma_t(x_{t:T}^{(i)}) / [\gamma_t(x_{t+1:T}) q(x_t^{(i)} | x_{t+1}^{(i)})]$.

The final set of weighted particles forms a discrete approximation to the final target γ_0 , which is asymptotically exact given infinite particles under regularity conditions [19]. However, the efficacy of SMC greatly depends on the choice of intermediate proposals and targets – the closer these intermediate distributions are to the marginals of the final target, the more effective the SMC sampler.

3 Method

Our goal is to sample from a target distribution $\pi(x) = \frac{1}{Z} \tilde{\pi}(x)$, where $\tilde{\pi}(x)$ is the unnormalized target and the normalization constant $Z = \int \tilde{\pi}(x) dx$ is typically intractable. We develop Reverse Diffusion Sequential Monte Carlo (RDSMC), a diffusion-based SMC sampler targeting $\pi(x)$.

To establish the connection between diffusion models and SMC, we consider an extended target distribution over the trajectory $x_{0:T} = (x_0, \dots, x_T)$ by discretizing the forward process in Eq. (1),

$$\pi(x_{0:T}) = \pi(x_0) \prod_{t=1}^T p(x_t | x_{t-1}), \quad (4)$$

where $p(x_t | x_{t-1})$ represents the forward transition kernel. For convenience, we assume a uniform time discretization $0 = \tau_0 < \dots < \tau_T = 1$ with step size $\delta = \frac{1}{T}$, and set each $x_t := x(\tau_t)$. We also write $\alpha_t := \alpha(\tau_t)$, $\sigma_t := \sigma(\tau_t)$, $f_t := f(\tau_t)$, $g_t := g(\tau_t)$ for time-dependent coefficients, and denote the marginal at step t by $p(x_t) := p_\tau(x(\tau_t))$ and the posterior by $p(x_0 | x_t) := p_\tau(x(0) | x(\tau_t))$.

The extended target $\pi(x_{0:T})$ admits a sequential factorization and preserves the desired marginal $\pi(x_0)$ at the final step $t = 0$, enabling the application of SMC. In § 3.1, we first introduce a reverse diffusion proposal that approximately samples from the extended target. Building on prior work, the proposal simulates a reverse diffusion process using Monte Carlo (MC) estimates of the score, which introduce auxiliary variables $u_{0:T}$ to represent randomness in estimates. In § 3.2, we construct informative intermediate targets over all variables $\{x_{t:T}, u_{t:T}\}$ to correct for proposal bias. These targets account for auxiliary randomness, and approximate the ideal ones using byproducts of the score estimation. Finally in § 3.3, we present the full RDSMC algorithm and its theoretical guarantees.

3.1 Reverse diffusion proposal

We devise a sequence of intermediate proposal distributions based on the discretized reverse diffusion process using MC estimates of the score. A crucial component is the explicit treatment of the auxiliary randomness introduced by score estimation, which we model jointly with the diffusion dynamics. The resulting proposal is an extended distribution over both diffusion states and auxiliary variables.

Monte Carlo score estimation. We first define a generic MC estimator $s(x_t, \mathbf{u}_t)$ of the score function based on the denoising score identity in Eq. (3), where \mathbf{u}_t denotes the randomness in estimation.

As an illustrative example, consider an importance sampling (IS) estimator (see Algorithm 2). Given x_t , we use a proposal $\mathcal{N}(\cdot | x_t/\alpha_t, \sigma_t^2/\alpha_t^2 \mathbb{I})$ obtained by reversing the forward transition kernel. The score can then be estimated by drawing M samples $\mathbf{u}_t = \{u_t^{(1)}, \dots, u_t^{(M)}\}$ from this proposal:

$$\nabla_{x_t} \log p(x_t) \approx s(x_t, \mathbf{u}_t) := \sum_{m=1}^M \frac{w^{(m)}}{\sum_{m'=1}^M w^{(m')}} \cdot \frac{\alpha_t u_t^{(m)} - x_t}{\sigma_t^2}, \quad (5)$$

where the importance weights are given by

$$w^{(m)} = \frac{\tilde{\pi}(u_t^{(m)}) \mathcal{N}(x_t | \alpha_t u_t^{(m)}, \sigma_t^2 I)}{\mathcal{N}(u_t^{(m)} | x_t/\alpha_t, \sigma_t^2/\alpha_t^2 \mathbb{I})}, \quad m = 1, \dots, M. \quad (6)$$

More informative IS proposals or advanced MC methods such as AIS or SMC can be used to improve score estimates. Other score identities may also be leveraged. See Appendix B.1 for further details.

For generality, we define \mathbf{u}_t as the collection of *all* auxiliary random variables generated during the MC score estimation at step t , with sampling distribution $q(\mathbf{u}_t | x_t)$. The density $q(\mathbf{u}_t | x_t)$ need not be evaluated. We denote the resulting score estimator as $s(x_t, \mathbf{u}_t)$.

Discretizing reverse diffusion. With the score estimator in place, we approximate the discretized transition kernel of the reverse SDE in Eq. (2) at step t by

$$q(x_t | x_{t+1}, \mathbf{u}_{t+1}) := \mathcal{N}(x_t | x_{t+1} - [f_{t+1} x_{t+1} - g_{t+1}^2 s(x_{t+1}, \mathbf{u}_{t+1})] \delta, g_{t+1}^2 \delta). \quad (7)$$

Extended proposal distributions. The full sampling process begins with drawing x_T from the reference distribution $q(x_T) := p(x_T)$, followed by iteratively refining x_t through the reverse kernel $q(x_t | x_{t+1}, \mathbf{u}_{t+1})$ in Eq. (7). At each iteration, the auxiliary variable $\mathbf{u}_t \sim q(\mathbf{u}_t | x_t)$ is introduced to estimate the score $s(x_t, \mathbf{u}_t)$. This process defines a proposal over the extended space of $\{x_t, \mathbf{u}_t\}_{t=0}^T$,

$$q(x_{0:T}, \mathbf{u}_{0:T}) = q(x_T) q(\mathbf{u}_T | x_T) \prod_{t=0}^{T-1} q(x_t | x_{t+1}, \mathbf{u}_{t+1}) q(\mathbf{u}_t | x_t). \quad (8)$$

While sampling \mathbf{u}_0 at the final step $t = 0$ is not necessary, we retain it for notation simplicity.

This sampling procedure builds on the prior work of Huang et al. [8], Grenioux et al. [9], which estimates the score function using MCMC. In contrast, we specifically adopt an IS- or SMC-based score estimate that also provides an unbiased estimate of the normalization constant. This property will be leveraged in the next section to construct intermediate target distributions for SMC.

3.2 Intermediate targets

Samples from the reverse diffusion proposal deviate from the true target due to two sources of error: time discretization of the reverse SDE, and bias in score estimation. To correct for these discrepancies, we design a series of intermediate target distributions. We first characterize the optimal but intractable targets, and then develop practical approximations using byproducts of score estimation. Finally, we extend the intermediate targets to include auxiliary variables. Our construction aligns with the ideal targets at intermediate steps and recovers the desired marginal $\pi(x_0)$ at the final step $t = 0$.

Optimal intermediate targets. The optimal intermediate target at step t is the marginal distribution of the extended target $\pi(x_{0:T})$ defined in Eq. (4):

$$\gamma_t^*(x_{t:T}) = \int \pi(x_{0:T}) dx_{0:t-1} = p(x_t) \prod_{i=t+1}^T p(x_i | x_{i-1}). \quad (9)$$

This choice is optimal as it leads to exact samples from $\pi(x_0)$ with locally optimal proposals [22].

However, the marginal $p(x_t) = \int \pi(x_0) \mathcal{N}(x_t | \alpha_t x_0, \sigma_t^2 \mathbb{I}) dx_0$ in Eq. (9) involves an intractable integral, except in the final step $t = 0$, where $p(x_0) = \pi(x_0)$ is known up to a normalization constant.

Approximating the marginal. At step $t > 0$, we approximate the marginal distribution $p(x_t)$ by $\hat{p}(x_t, \mathbf{u}_t)$ using the same auxiliary variables \mathbf{u}_t used for the score estimation. The key insight is that $Zp(x_t)$ is the normalization constant of the posterior $p(x_0 | x_t) \propto \tilde{\pi}(x_0) \mathcal{N}(x_t | \alpha_t x_0, \sigma_t^2 \mathbb{I})$. Thus, by performing IS (or a similar AIS / SMC procedure) targeting $p(x_0 | x_t)$, we obtain importance weights $\{w^{(m)}\}_{m=1}^M$ that provide an unbiased estimate of $p(x_t)$ up to the normalization constant Z . We define

$$\hat{p}(x_t, \mathbf{u}_t) := \frac{1}{M} \sum_{m=1}^M w^{(m)}, \text{ where we have } \mathbb{E}_{q(\mathbf{u}_t | x_t)} [\hat{p}(x_t, \mathbf{u}_t)] = Zp(x_t). \quad (10)$$

At the final step $t = 0$, we set $\hat{p}(x_0, \mathbf{u}_0) := \tilde{\pi}(x_0) = Z\pi(x_0)$ as no approximation is needed.

See Algorithm 2 for an example of utilizing the earlier IS score estimator to compute $\hat{p}(x_t, \mathbf{u}_t)$.

Extended intermediate targets. Finally, we incorporate the auxiliary variables by setting the targets to match their sampling distributions and define the intermediate target over $\{x_{t:T}, \mathbf{u}_{t:T}\}$ as

$$\gamma_t(x_{t:T}, \mathbf{u}_{t:T}) := \hat{p}(x_t, \mathbf{u}_t) q(\mathbf{u}_t | x_t) \prod_{i=t}^{T-1} p(x_{i+1} | x_i) q(\mathbf{u}_{i+1} | x_{i+1}) \quad (11)$$

for $t = 0, \dots, T-1$, and $\gamma_T(x_T, \mathbf{u}_T) := \hat{p}(x_T, \mathbf{u}_T) q(\mathbf{u}_T | x_T)$.

The structure in Eq. (11) mirrors the optimal target in Eq. (9), replacing the intractable $p(x_t)$ with an unbiased estimate $\hat{p}(x_t, \mathbf{u}_t)$ (up to a factor of Z) and accounting for auxiliary randomness. In fact, marginalizing out the auxiliary variables $\mathbf{u}_{t:T}$ in $\gamma_t(x_{t:T}, \mathbf{u}_{t:T})$ recovers the optimal target

$$\begin{aligned} \int \gamma_t(x_{t:T}, \mathbf{u}_{t:T}) d\mathbf{u}_{t:T} &= \mathbb{E}_{q(\mathbf{u}_t | x_t)} [\hat{p}(x_t, \mathbf{u}_t)] \prod_{i=t}^{T-1} p(x_{i+1} | x_i) \\ &= Zp(x_t) \prod_{i=t}^{T-1} p(x_{i+1} | x_i) \propto \gamma_t^*(x_{t:T}), \end{aligned} \quad (12)$$

where the last line follows from the unbiasedness property in Eq. (10), for any step $t > 0$. This is often referred to as an *exact approximation* [21, 22], as we still target the true γ_t^* despite the approximation.

Crucially, the marginal of the final target $\gamma_0(x_0)$ matches the desired target $\pi(x_0)$,

$$\gamma_0(x_0) = \int \tilde{\pi}(x_0) \prod_{i=1}^T p(x_i | x_{i-1}) q(\mathbf{u}_i | x_i) dx_{1:T}, \mathbf{u}_{0:T} \propto \pi(x_0), \quad (13)$$

as $\hat{p}(x_0, \mathbf{u}_0) = \tilde{\pi}(x_0)$ is exact by construction.

The observations from Eqs. (12) and (13) ensure that the SMC procedure we describe next provides effective guidance at intermediate steps while correctly targeting the final distribution.

3.3 RDSMC: Algorithm and theoretical guarantee

With the proposals and intermediate targets in place, we now derive tractable weighting functions. Finally, we present the complete RDSMC algorithm and establish its theoretical guarantees.

Algorithm 1: Reverse Diffusion Sequential Monte Carlo (RDSMC)

Input: Unnormalized target $\tilde{\pi}(x_0)$, number of particles N , discretization steps T , score estimation budget M , diffusion schedule $\{\alpha_t, \sigma_t, f_t, g_t\}$ and reference distribution $p(x_T)$

Output: Weighted samples $\{x_0^{(i)}, w_0^{(i)}\}_{i=1}^N$ and normalization constant estimate \hat{Z}

```

1 for  $i \leftarrow 1$  to  $N$  do
2   Sample  $x_T^{(i)} \sim p(x_T)$ ;
3   Compute score and marginal estimates  $s_T^{(i)}, \hat{p}_T^{(i)} \leftarrow \text{Algorithm 2}(\pi, \alpha_T, \sigma_T, x_T^{(i)}, M)$ ;
4   Compute weight:  $w_T^{(i)} \leftarrow \frac{\hat{p}_T^{(i)}}{p(x_T^{(i)})}$ ;
5 for  $t \leftarrow T-1$  to  $0$  do
6   Resample  $\{x_{t+1}^{(i)}, \mathbf{u}_{t+1}^{(i)}, s_{t+1}^{(i)}, \tilde{\pi}_{t+1}^{(i)}\}_{i=1}^N$  according to weights  $\{w_{t+1}^{(i)}\}_{i=1}^N$  ;
7   for  $i \leftarrow 1$  to  $N$  do
8     Sample  $x_t^{(i)} \sim q(x_t \mid x_{t+1}^{(i)}, \mathbf{u}_{t+1}^{(i)}) := \mathcal{N}\left(x_t \mid x_{t+1}^{(i)} - \left[f_{t+1}x_{t+1}^{(i)} - g_{t+1}^2 s_{t+1}^{(i)}\right] \delta, g_{t+1}^2 \delta\right)$ ;
9     if  $t > 0$  then
10       Compute score and marginal estimates  $s_t^{(i)}, \hat{p}_t^{(i)} \leftarrow \text{Algorithm 2}(\pi, \alpha_t, \sigma_t, x_t^{(i)}, M)$ ;
11     else
12       Compute exact marginal  $\hat{p}_0^{(i)} \leftarrow \tilde{\pi}(x_0^{(i)})$ ;
13     Compute weight:  $w_t^{(i)} \leftarrow \frac{\hat{p}_t^{(i)} p(x_{t+1}^{(i)} \mid x_t^{(i)})}{\hat{p}_{t+1}^{(i)} q(x_t^{(i)} \mid x_{t+1}^{(i)}, \mathbf{u}_{t+1}^{(i)})}$ ;
14 Compute normalization constant estimate  $\hat{Z} \leftarrow \prod_{t=0}^T \frac{1}{N} \sum_{i=1}^N w_t^{(i)}$ .

```

Weighting functions. For $t = T-1, \dots, 0$, the intermediate weight is computed as:

$$w_t = \frac{\gamma_t(x_{t:T}, \mathbf{u}_{t:T})}{\gamma_{t+1}(x_{t+1:T}, \mathbf{u}_{t+1:T}) q(x_t \mid x_{t+1}, \mathbf{u}_{t+1}) q(\mathbf{u}_t \mid x_t)}, \quad (14)$$

substituting intermediate target expressions from Eq. (11) and canceling out common terms, we obtain

$$w_t = \frac{\hat{p}(x_t, \mathbf{u}_t) p(x_{t+1} \mid x_t)}{\hat{p}(x_{t+1}, \mathbf{u}_{t+1}) q(x_t \mid x_{t+1}, \mathbf{u}_{t+1})}. \quad (15)$$

At the initial step T , the weight is $w_T = \frac{\gamma_T(x_T, \mathbf{u}_T)}{q(x_T) q(\mathbf{u}_T \mid x_T)} = \frac{\hat{p}(x_T, \mathbf{u}_T)}{p(x_T)}$.

Notably, although the intermediate proposals and targets involve auxiliary sampling distributions, the weighting functions remain tractable and agnostic to them. This result allows the use of a fairly generic auxiliary sampler for score and marginal estimation, while still yielding computable weights.

The RDSMC algorithm and theoretical guarantees. We summarize the RDSMC algorithm in Algorithm 1. It initializes N particles from the reference distribution. Subsequently, the particles are propagated through a diffusion-based proposal, followed by reweighting and resampling using intermediate targets. These steps are enabled by MC sampling from the posterior $p(x_0 \mid x_t)$. The final output is a weighted set of samples approximating the target $\pi(x)$, along with an estimate of the normalization constant Z . While Algorithm 1 uses IS from Algorithm 2 for MC sampling, RDSMC can incorporate more advanced AIS or SMC methods. See Appendix B.1 for details.

RDSMC can be viewed as an adaptation of the *nested* SMC framework [23, 28]. Specifically, each particle at step t involves running an inner-level MC estimator to compute the score function and the marginal density. This inner estimator constitutes an IS or a similar procedure that targets the posterior distribution $p(x_0 \mid x_t)$, which is then used to assign *proper weights* [22, Chapter 4.3] to proposed samples x_t . Consequently, the proposed RDSMC framework naturally inherits the unbiasedness and asymptotic exactness guarantees of such SMC algorithms [23, 22].

Theorem 1. *The RDSMC algorithm provides a consistent estimator of the target distribution $\pi(x_0)$ as particle size $N \rightarrow \infty$ and an unbiased estimator of the normalization constant Z for any $N \geq 1$.*

We provide the formal statement and proof in Appendix C, under standard regularity assumptions.

4 Related works

Training-free diffusion-based samplers. Huang et al. [8] develops a sampling algorithm based on the reverse SDE of an Ornstein-Uhlenbeck process, using MCMC to estimate the score function. This method, in contrast to RDSMC, initializes the reverse process at an earlier time $\tau_T < 1$, where initial samples are obtained via a nested Langevin procedure. Grenioux et al. [9] considers a similar stochastic localization scheme. They further adapt the time discretization of the SDE to its signal-to-noise ratio (SNR) profile, and provide guidance on choosing the initial sampling time τ_T given certain target conditions.

While Huang et al. [8] provides an upper bound on the sample complexity, their practical performance can be hindered by finite time discretization and score approximation biases. RDSMC wraps similar diffusion-based samplers as a proposal within a principled SMC framework. By introducing novel intermediate targets, we systematically correct for discretization and score estimation errors and provide an unbiased estimate of the normalization constant.

Diffusion-based neural samplers. A separate line of work on neural samplers trains diffusion model for sampling. Variational approaches achieve this goal by minimizing the divergence between forward and reverse processes [13, 14, 16, 17, 15], while Akhoud-Sadegh et al. [11], OuYang et al. [12] exploit analytic expressions of the score function or a related energy function. Similar to their training-free counterparts, these methods are prone to discretization and approximation errors.

Closest to our work are Phillips et al. [10], Chen et al. [18] that also use SMC to reduce errors in neural samplers. Unlike our method, their proposals require training. Phillips et al. [10] construct intermediate targets using a learned neural network approximation, while ours are training-free and reflect the true target marginals at each SMC iteration. Chen et al. [18] define the extended target along a geometric annealing path, while we derive ours from the forward process of diffusion models.

Recently, He et al. [20] show that neural samplers typically incur heavy computational overhead and rely on specific network conditioning, compared to classical sampling methods. For this reason, we limit our empirical comparison to training-free samplers. Nonetheless, an interesting direction for future work is to combine our method with training-based approaches to further enhance performance.

SMC for conditional generation from diffusion models. Beyond classical sampling tasks, SMC has been applied to conditional generation for pre-trained diffusion models [29, 30, 31, 32]. While these works also combine SMC and diffusion dynamics, a key distinction is the target distribution: they sample from an existing diffusion model prior tilted with a reward function, whereas our setting involves sampling from any (unnormalized) target distribution. As a result, the way diffusion models are used is different, and we require distinct designs for proposals and intermediate targets in SMC.

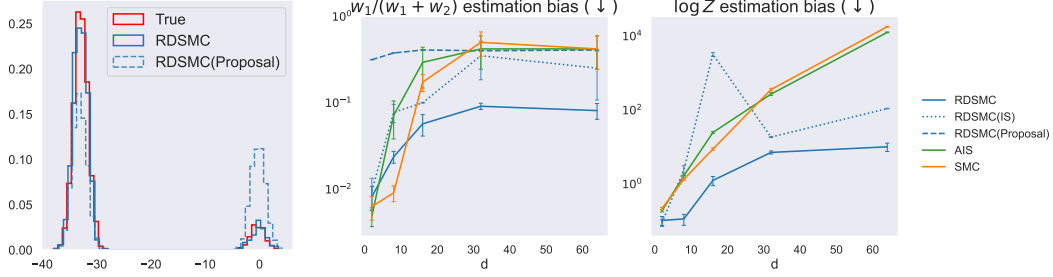
5 Experiments

We evaluate RDSMC on a range of synthetic and real-world target distributions, comparing it to SMC [25], AIS [24], SMS [33], RDMC [8], and SLIPS [9]. AIS and SMC operate over a series of geometric interpolations between the target and a Gaussian proposal with MCMC transitions. SMS samples from the target by sequentially denoising equally noised measurements using a Langevin procedure combined with estimated scores. RDMC and SLIPS are described in § 4.

RDSMC uses a variance-preserving diffusion schedule with annealed importance sampling for score estimation. To evaluate the effectiveness of intermediate target distributions and importance of the resampling mechanism, we include two ablations: (i) RDSMC (Proposal), which samples directly from the reverse diffusion proposal in Eq. (8) without any weighting or resampling, and (ii) RDSMC (IS), which applies a final IS correction to samples from RDSMC (Proposal).

Baseline methods follow the implementation of Grenioux et al. [9]. Notably, the information about the target variance (or an estimation) is provided to guide the initialization of the baselines SMC, AIS, SMS and SLIPS. In contrast, our method does *not* make use of this information.

Unless otherwise specified, we use $T = 100$ discretization steps for RDSMC and its variants, and $T = 1,024$ steps for other methods. We generate $N = 4,096$ final samples for all methods, and



(a) $d = 2$: histogram along 1st dimension. While RDSMC's proposal covers the modes, the SMC procedure is crucial for producing calibrated weights.

(b) Estimation bias of weight ratio $w_1/(w_1 + w_2)$ and log-normalization constant $\log Z$ versus dimension d . Results are averaged over 5 seeds with error bars showing one standard error. Bias increases with d for all methods, while RDSMC consistently outperforms the baselines. SMS, RDMC, and SLIPS results are shown in Appendix D.2 and exhibit consistently higher bias.

Figure 1: Bi-modal Gaussian mixture study.

tune their hyperparameters assuming access to either a validation dataset or an oracle metric. All experiment details are included in Appendix D.

5.1 Bi-modal gaussian mixtures

We first study bi-modal Gaussian mixtures with an imbalanced weight ratio of $w_1/(w_1 + w_2) = 0.1$ for varying dimensions d . The estimated ratio is obtained by assigning samples to the mode with the highest posterior probability. For each method we report the result with the lowest estimation bias.

In Figure 1a, we compare the marginal histogram of samples from RDSMC, RDSMC (Proposal), and the true target in $d = 2$. While samples from RDSMC (Proposal) cover both modes, their relative weights are overly balanced. In contrast, RDSMC recovers the calibrated mode weights, indicating the importance of the error correction mechanism by SMC.

Figure 1b shows the estimation bias of the weight ratio (left), and that of the log-normalization constant $\log Z$ (right). RDSMC consistently outperforms AIS and SMC in both metrics across dimensions. RDSMC (Proposal) exhibits consistently high weight ratio estimation bias. While RDSMC (IS) reduces this bias, it still underperforms the full RDSMC procedure, highlighting the effectiveness of intermediate resampling guided by our intermediate target distributions.

In high dimensions, all methods exhibit some degree of mode collapse. RDSMC primarily samples from the dominant mode, resulting in average weight ratio estimation biases of 0.09 and 0.08 for $d = 32$ and 64, respectively. In contrast, AIS and SMC completely collapse to a single mode, which varies across runs, yielding degenerate estimated ratios of 0 or 1 and an average bias of around 0.4.

Results for SMS, RDMC, and SLIPS are included in Appendix D.2, which show higher weight ratio estimation bias compared to RDSMC. Additionally, they do not provide estimates for $\log Z$.

5.2 Rings and Funnel distributions

We present results on two additional synthetic targets. Rings, introduced by Grenioux et al. [9], is a 2-dimensional distribution constructed via an inverse polar parameterization: the angular component is uniformly distributed, while the radius component follows a 4-mode Gaussian mixture. We assess sample quality using total variational distance in the radius component (radius TVD). Funnel, proposed by Neal [34], is a 10-dimensional “funnel”-shaped distribution. We use sliced Kolmogorov-Smirnov distance (sliced KSD) to evaluate sample quality following Grenioux et al. [9]. Both targets admit tractable normalization constants, so we also report the estimation bias for methods that compute it. For each method, we show results with the highest sample quality on a validation dataset.

As shown in Table 1, RDSMC achieves lower or comparable estimation bias of the log-normalization constant relative to AIS and SMC on both targets. On the simpler Rings target, RDSMC (Proposal) has the lowest radius TVD, where AIS, SMC and RDSMC closely match. On the more challenging

Algorithm	Rings ($d = 2$)		Funnel ($d = 10$)	
	Radius TVD (\downarrow)	$\log Z$ Bias (\downarrow)	Sliced KSD (\downarrow)	$\log Z$ Bias (\downarrow)
AIS	0.10 ± 0.00	0.05 ± 0.00	0.07 ± 0.00	0.28 ± 0.01
SMC	0.10 ± 0.00	0.05 ± 0.00	0.07 ± 0.00	0.28 ± 0.01
SMS	0.24 ± 0.01	N/A	0.15 ± 0.00	N/A
RDMC	0.37 ± 0.00	N/A	0.13 ± 0.00	N/A
SLIPS	0.19 ± 0.00	N/A	0.06 ± 0.00	N/A
RDSMC	0.13 ± 0.01	0.03 ± 0.00	0.11 ± 0.00	0.28 ± 0.10
RDSMC(IS)	0.15 ± 0.01	0.02 ± 0.01	0.33 ± 0.03	1.61 ± 0.14
RDSMC(Proposal)	0.09 ± 0.00	N/A	0.32 ± 0.03	N/A

Table 1: Synthetic target results (mean \pm standard error over 5 seeds). Bold indicates 95% confidence interval overlap with that of the best average result. RDSMC consistently yields the lowest $\log Z$ estimation bias. On Rings, RDSMC(Proposal) has the lowest radius TVD, followed by AIS, SMC, and RDSMC. On Funnel, SLIPS has the lowest sliced KSD, followed by AIS, SMC, and RDSMC.

Test LL (\uparrow)	Credit ($d = 25$)	Cancer ($d = 31$)	Ionosphere ($d = 35$)	Sonar ($d = 61$)
AIS	-122.73 ± 0.51	-60.45 ± 0.31	-86.37 ± 0.10	-110.11 ± 0.06
SMC	-123.17 ± 0.05	-60.28 ± 0.11	-86.37 ± 0.10	-110.11 ± 0.06
SMS	-527.79 ± 0.85	-215.64 ± 0.66	-202.56 ± 0.16	-275.44 ± 0.31
RDMC	-388.24 ± 1.75	-182.81 ± 0.43	-108.67 ± 0.09	-128.29 ± 0.03
SLIPS	-121.79 ± 0.04	-56.26 ± 0.08	-85.07 ± 0.07	-102.39 ± 0.03
RDSMC	-124.00 ± 1.96	-62.23 ± 1.96	-87.72 ± 1.75	-101.52 ± 1.84
RDSMC(IS)	-144.38 ± 4.63	-82.47 ± 7.78	-84.90 ± 2.84	-110.57 ± 4.54
RDSMC(Proposal)	-606.03 ± 1.26	-246.86 ± 0.97	-92.62 ± 0.04	-134.72 ± 0.13

Table 2: Bayesian logistic regression with test log-likelihood (mean \pm standard error) averaged over 5 seeds. Bold indicates 95% confidence interval overlap with that of the best average result. SLIPS achieves the best overall performance, while RDSMC matches or closely approaches it. In contrast, RDSMC(Proposal) performs noticeably worse, highlighting the effectiveness of the SMC correction.

Funnel target, SLIPS achieves the lowest sliced KSD; while RDSMC performs slightly worse, it greatly outperforms its IS and Proposal variants. Additional results are provided in Appendix D.3.

5.3 Bayesian logistic regression

Finally, we evaluate inference performance on Bayesian logistic regression models using four datasets. Credit and Cancer [35] involve predicting credit risk and breast cancer recurrence, while Ionosphere [36] and Sonar [37] focus on classifying radar and sonar signals, respectively. The inference is performed on 60% of each dataset, leaving 20% for validation and 20% for testing. Each method is tuned using the validation log-likelihood estimate. We report the test log-likelihood in Table 2.

RDSMC achieves the best or near-best performance across datasets, closely matching SLIPS, which performs the best overall. This comparison suggests that SLIPS’s time discretization and initialization strategy may offer complementary benefits despite lacking systematic error correction. RDSMC (IS) underperforms on Credit and Cancer and exhibits higher variance than RDSMC, while RDSMC (Proposal) performs the worst, again highlighting the importance of the SMC mechanism. Compared to baseline methods, RDSMC shows greater variance, likely due to auxiliary randomness in its nested structure, suggesting a direction for future improvement.

6 Discussion

This paper presents a training-free and diffusion-based SMC sampler, Reverse Diffusion Sequential Monte Carlo (RDSMC), for sampling from unnormalized distributions. By leveraging reverse diffusion dynamics as proposals, we devise informative intermediate targets to correct systematic errors within a principled SMC framework. These components rely on Monte Carlo score estimation,

without requiring additional training. Our algorithm provides asymptotically exact samples from the target distribution and a finite-sample unbiased estimate of the normalization constant. Empirical results on both synthetic and Bayesian inference tasks demonstrate competitive or superior performance compared to existing diffusion-based and classical geometric annealing-based samplers.

Limitations and future work. As a nested SMC procedure, our proposed method inherently introduces auxiliary variance. Such variance may be mitigated by enhancing autocorrelation within the Monte Carlo estimation step, in the spirit of [38]. In high-dimensional Gaussian mixture experiments, we observe a degree of mode collapse, an issue also seen in other samplers. Potential remedies include adopting partial resampling strategies [39], or incorporating target information into our procedure. Our method also relies on hyperparameter tuning guided by oracle metrics, which aligns with common practice in the related literature. While heuristics aid in this process, developing a more automated strategy remains an important future direction. Finally, to further improve performance, we can incorporate SNR-adapted discretization schemes and informative initializations, as explored by Grenioux et al. [9], as well as combine our approach with diffusion-based neural samplers.

References

- [1] Christophe Andrieu, Nando De Freitas, Arnaud Doucet, and Michael I Jordan. An introduction to mcmc for machine learning. *Machine learning*, 50:5–43, 2003.
- [2] Christian P Robert, George Casella, Christian P Robert, and George Casella. The metropolis—hastings algorithm. *Monte Carlo statistical methods*, pages 267–320, 2004.
- [3] Daan Frenkel and Berend Smit. Molecular simulation: from algorithms to applications, 2000.
- [4] Sourav Chatterjee and Persi Diaconis. The sample size required in importance sampling. *The Annals of Applied Probability*, 28(2):1099–1135, 2018.
- [5] David M Blei, Alp Kucukelbir, and Jon D McAuliffe. Variational inference: A review for statisticians. *Journal of the American statistical Association*, 112(518):859–877, 2017.
- [6] Jonathan Ho, Ajay Jain, and Pieter Abbeel. Denoising diffusion probabilistic models. *Advances in neural information processing systems*, 33:6840–6851, 2020.
- [7] Yang Song, Jascha Sohl-Dickstein, Diederik P Kingma, Abhishek Kumar, Stefano Ermon, and Ben Poole. Score-based generative modeling through stochastic differential equations. *arXiv preprint arXiv:2011.13456*, 2020.
- [8] Xunpeng Huang, Hanze Dong, Yifan Hao, Yi-An Ma, and Tong Zhang. Reverse diffusion monte carlo. *arXiv preprint arXiv:2307.02037*, 2023.
- [9] Louis Grenioux, Maxence Noble, Marylou Gabrié, and Alain Oliviero Durmus. Stochastic localization via iterative posterior sampling. *arXiv preprint arXiv:2402.10758*, 2024.
- [10] Angus Phillips, Hai-Dang Dau, Michael John Hutchinson, Valentin De Bortoli, George Deli-giannidis, and Arnaud Doucet. Particle denoising diffusion sampler. In *Forty-first International Conference on Machine Learning*, 2024.
- [11] Tara Akhound-Sadegh, Jarrid Rector-Brooks, Avishek Joey Bose, Sarthak Mittal, Pablo Lemos, Cheng-Hao Liu, Marcin Sendera, Siamak Ravanbakhsh, Gauthier Gidel, Yoshua Bengio, et al. Iterated denoising energy matching for sampling from boltzmann densities. *arXiv preprint arXiv:2402.06121*, 2024.
- [12] RuiKang OuYang, Bo Qiang, Zixing Song, and José Miguel Hernández-Lobato. Bnem: A boltzmann sampler based on bootstrapped noised energy matching. *arXiv preprint arXiv:2409.09787*, 2024.
- [13] Qinsheng Zhang and Yongxin Chen. Path Integral Sampler: a stochastic control approach for sampling. In *The Tenth International Conference on Learning Representations*, 2022.
- [14] Julius Berner, Lorenz Richter, and Karen Ullrich. An optimal control perspective on diffusion-based generative modeling. *Transactions on Machine Learning Research*, 2023.

[15] Lorenz Richter, Julius Berner, and Guan-Horng Liu. Improved sampling via learned diffusions. In *ICML Workshop on New Frontiers in Learning, Control, and Dynamical Systems*, 2023.

[16] Francisco Vargas, Will Sussman Grathwohl, and Arnaud Doucet. Denoising diffusion samplers. In *The Eleventh International Conference on Learning Representations*, 2023.

[17] Francisco Vargas, Shreyas Padhy, Denis Blessing, and Nikolas Nüsken. Transport meets variational inference: Controlled monte carlo diffusions. In *The Twelfth International Conference on Learning Representations*, 2024.

[18] Junhua Chen, Lorenz Richter, Julius Berner, Denis Blessing, Gerhard Neumann, and Anima Anandkumar. Sequential controlled langevin diffusions. *arXiv preprint arXiv:2412.07081*, 2024.

[19] Nicolas Chopin and Omiros Papaspiliopoulos. *An introduction to sequential Monte Carlo*. Springer, 2020.

[20] Jiajun He, Yuanqi Du, Francisco Vargas, Dinghuai Zhang, Shreyas Padhy, RuiKang OuYang, Carla Gomes, and José Miguel Hernández-Lobato. No trick, no treat: Pursuits and challenges towards simulation-free training of neural samplers. *arXiv preprint arXiv:2502.06685*, 2025.

[21] Christophe Andrieu, Arnaud Doucet, and Roman Holenstein. Particle markov chain monte carlo methods. *Journal of the Royal Statistical Society Series B: Statistical Methodology*, 72(3):269–342, 2010.

[22] Christian A Naesseth, Fredrik Lindsten, Thomas B Schön, et al. Elements of sequential monte carlo. *Foundations and Trends® in Machine Learning*, 12(3):307–392, 2019.

[23] Christian Naesseth, Fredrik Lindsten, and Thomas Schon. Nested sequential monte carlo methods. In *International Conference on Machine Learning*, pages 1292–1301. PMLR, 2015.

[24] Radford M Neal. Annealed importance sampling. *Statistics and computing*, 11:125–139, 2001.

[25] Pierre Del Moral, Arnaud Doucet, and Ajay Jasra. Sequential monte carlo samplers. *Journal of the Royal Statistical Society Series B: Statistical Methodology*, 68(3):411–436, 2006.

[26] Pascal Vincent. A connection between score matching and denoising autoencoders. *Neural computation*, 23(7):1661–1674, 2011.

[27] Bradley Efron. Tweedie’s formula and selection bias. *Journal of the American Statistical Association*, 106(496):1602–1614, 2011.

[28] Christian A Naesseth, Fredrik Lindsten, and Thomas B Schön. High-dimensional filtering using nested sequential monte carlo. *IEEE Transactions on Signal Processing*, 67(16):4177–4188, 2019.

[29] Brian L Trippe, Jason Yim, Doug Tischer, Tamara Broderick, David Baker, Regina Barzilay, and Tommi Jaakkola. Diffusion probabilistic modeling of protein backbones in 3D for the motif-scaffolding problem. In *International Conference on Learning Representations*, 2023.

[30] Luhuan Wu, Brian Trippe, Christian Naesseth, David Blei, and John P Cunningham. Practical and asymptotically exact conditional sampling in diffusion models. *Advances in Neural Information Processing Systems*, 36:31372–31403, 2023.

[31] Gabriel Cardoso, Yazid Janati El Idrissi, Sylvain Le Corff, and Eric Moulines. Monte carlo guided diffusion for bayesian linear inverse problems. *arXiv preprint arXiv:2308.07983*, 2023.

[32] Raghav Singhal, Zachary Horvitz, Ryan Teehan, Mengye Ren, Zhou Yu, Kathleen McKeown, and Rajesh Ranganath. A general framework for inference-time scaling and steering of diffusion models. *arXiv preprint arXiv:2501.06848*, 2025.

[33] Saeed Saremi, Ji Won Park, and Francis Bach. Chain of log-concave markov chains. *arXiv preprint arXiv:2305.19473*, 2023.

[34] Radford M Neal. Slice sampling. *The annals of statistics*, 31(3):705–767, 2003.

[35] Robert Nishihara, Iain Murray, and Ryan P Adams. Parallel mcmc with generalized elliptical slice sampling. *The Journal of Machine Learning Research*, 15(1):2087–2112, 2014.

[36] Vincent G Sigillito, Simon P Wing, Larrie V Hutton, and Kile B Baker. Classification of radar returns from the ionosphere using neural networks. *Johns Hopkins APL Technical Digest*, 10(3):262–266, 1989.

[37] R Paul Gorman and Terrence J Sejnowski. Analysis of hidden units in a layered network trained to classify sonar targets. *Neural networks*, 1(1):75–89, 1988.

[38] George Deligiannidis, Arnaud Doucet, and Michael K Pitt. The correlated pseudomarginal method. *Journal of the Royal Statistical Society Series B: Statistical Methodology*, 80(5):839–870, 2018.

[39] Luca Martino, Victor Elvira, and Francisco Louzada. Weighting a resampled particle in sequential monte carlo. In *2016 IEEE Statistical Signal Processing Workshop (SSP)*, pages 1–5. IEEE, 2016.

[40] Simo Särkkä and Arno Solin. *Applied stochastic differential equations*, volume 10. Cambridge University Press, 2019.

[41] Valentin De Bortoli, Michael Hutchinson, Peter Wirnsberger, and Arnaud Doucet. Target score matching, 2024.

[42] Jiajun He, Yuanqi Du, Francisco Vargas, Yuanqing Wang, Carla P. Gomes, José Miguel Hernández-Lobato, and Eric Vanden-Eijnden. Feat: Free energy estimators with adaptive transport, 2025.

[43] Jiajun He, Wenlin Chen, Mingtian Zhang, David Barber, and José Miguel Hernández-Lobato. Training neural samplers with reverse diffusive kl divergence. *arXiv preprint arXiv:2410.12456*, 2024.

[44] Gareth O Roberts and Richard L Tweedie. Geometric convergence and central limit theorems for multidimensional hastings and metropolis algorithms. *Biometrika*, 83(1):95–110, 1996.

[45] Radford M Neal. Mcmc using hamiltonian dynamics. *arXiv preprint arXiv:1206.1901*, 2012.

[46] Gareth O Roberts and Richard L Tweedie. Exponential convergence of langevin distributions and their discrete approximations. *Bernoulli*, 2(4):341–363, 1996.

[47] Maxence Noble, Louis Grenioux, Marylou Gabrié, and Alain Oliviero Durmus. Learned reference-based diffusion sampling for multi-modal distributions. *arXiv preprint arXiv:2410.19449*, 2024.

[48] Louis Grenioux, Alain Oliviero Durmus, Eric Moulines, and Marylou Gabrié. On sampling with approximate transport maps. In *Proceedings of the 40th International Conference on Machine Learning*, volume 202 of *Proceedings of Machine Learning Research*, pages 11698–11733. PMLR, 23–29 Jul 2023.

[49] Rémi Flamary, Nicolas Courty, Alexandre Gramfort, Mokhtar Z. Alaya, Aurélie Boisbunon, Stanislas Chambon, Laetitia Chapel, Adrien Corenflos, Kilian Fatras, Nemo Fournier, Léo Gautheron, Nathalie T.H. Gayraud, Hicham Janati, Alain Rakotomamonjy, Ievgen Redko, Antoine Rolet, Antony Schutz, Vivien Seguy, Danica J. Sutherland, Romain Tavenard, Alexander Tong, and Titouan Vayer. Pot: Python optimal transport. *Journal of Machine Learning Research*, 22(78):1–8, 2021.

A Background: diffusion models and diffusion-based samplers

A.1 Diffusion models

We review common diffusion schedules used in the literature.

Variance-preserving schedule. In Variance-Preserving (VP) schedule [6], the coefficients of the forward SDE in Eq. (1) are given by

$$f(\tau) = -\frac{1}{2}b(\tau), \quad g(\tau) = \sqrt{b(\tau)}, \quad (16)$$

where $b(\tau)$ is a time-dependent function

$$b(\tau) = b_{\min} + \tau(b_{\max} - b_{\min}),$$

for some constants $b_{\min} \approx 0 \ll b_{\max}$. For a large value of b_{\max} , the reference distribution is approximately standard normal, $p_1(x) \approx \mathcal{N}(x \mid 0, 1)$.

By Ito's calculus (see e.g. Särkkä and Solin [40]), one can show that the transition kernel $p_{\tau}(x(\tau) \mid x_0) = \mathcal{N}(x(\tau) \mid \alpha(\tau)x_0, \sigma(\tau)^2)$ with

$$\alpha(\tau) = \exp\left(-\frac{1}{2} \int_0^{\tau} b(s)ds\right), \quad \sigma(\tau)^2 = 1 - \exp\left(-\int_0^{\tau} b(s)ds\right).$$

Variance-exploding schedule. In Variance-Exploding (VE) schedule [7], the forward SDE coefficients in Eq. (1) are given by

$$f(\tau) = 0, \quad g(\tau) = \sqrt{\frac{d\sigma^2(\tau)}{d\tau}},$$

where $\sigma(\tau)$ is a non-negative and monotone increasing function with $\sigma(0) = 0$. Commonly used forms of $\sigma(\tau)$ include polynomial functions, such as linear, quadratic or exponential schedules. When $\sigma(1)$ is large, the reference distribution can be effectively approximated as $p_1(x) \approx \mathcal{N}(x \mid 0, \sigma(1)^2)$.

Similarly to the VP case, one can derive the following parameters of the Gaussian transition kernel $p_{\tau}(x(\tau) \mid x_0)$ with $\alpha(\tau) = 1$ and $\sigma(\tau)$ some non-negative and monotone function.

A.2 Diffusion-based samplers and score identities

Target score identity (TSI) TSI utilizes known structural properties of the target density, such as estimated gradients, facilitating potentially more accurate and lower-variance score estimations at low-noise settings. Formally, the score function of the noisy target distribution $p_{\tau}(x)$ under the TSI framework satisfies

$$\nabla_x \log p_{\tau}(x) = \frac{1}{\alpha(\tau)} \int \nabla_x \log p_{\tau}(x_0) p_{\tau}(x_0 \mid x) dx_0. \quad (17)$$

TSI and its related alternative have been used in several recent studies to improve score estimation accuracy [41, 10, 11, 42].

Mixed score identity (MSI) To balance the advantages of DSI and TSI across different noise regimes, MSI combines both identities through a convex interpolation. Specifically, MSI favors TSI in the low-noise regime and DSI in the high-noise regime, leveraging both strengths. Formally, MSI is a convex combination of TSI and DSI with coefficients $\frac{\alpha(\tau)^2}{\alpha(\tau)^2 + \sigma(\tau)^2}$ and $\frac{\sigma(\tau)^2}{\alpha(\tau)^2 + \sigma(\tau)^2}$:

$$\nabla_x \log p_{\tau}(x) = \frac{1}{\alpha(\tau)^2 + \sigma(\tau)^2} \int \left(\alpha(\tau)(x_0 + \nabla_x \log p_{\tau}(x_0)) - x(\tau) \right) p_{\tau}(x_0 \mid x) dx_0. \quad (18)$$

He et al. [43] leverage MSI to train an implicit generative model that produces samples in a single step, demonstrating improved sample quality and efficiency.

Algorithm 2: Importance sampler of $p(x_0 \mid x_t) \propto \tilde{\pi}(x_0) \mathcal{N}(x_t \mid \alpha_t x_0, \sigma_t^2 \mathbb{I})$

Input: Unnormalized prior $\tilde{\pi}(\cdot)$, likelihood parameters $\{\alpha_t, \sigma_t\}$, data x_t , and compute budget (number of importance samples) M .

Output: Score estimate $s(x_t, \mathbf{u}_t)$ and marginal estimate $\hat{p}(x_t, \mathbf{u}_t)$.

- 1 Sample $\mathbf{u}_t := \mathbf{u}_t^{(0:M)}$ i.i.d. from some proposal q ;
- 2 Compute importance weights: $w^{(m)} \leftarrow \frac{\tilde{\pi}(\mathbf{u}_t^{(m)}) \mathcal{N}(x_t \mid \alpha_t \mathbf{u}_t^{(m)}, \sigma_t^2 I)}{q(\mathbf{u}_t^{(m)})}$ for $m = 1, \dots, M$;
- 3 Compute score estimate: $s(x_t, \mathbf{u}_t) \leftarrow \sum_{m=1}^M \frac{w^{(m)}}{\sum_{m'=1}^M w^{(m')}} \cdot \frac{\alpha_t \mathbf{u}_t^{(m)} - x_t}{\sigma_t^2}$;
- 4 Compute marginal estimate: $\hat{p}(x_t, \mathbf{u}_t) \leftarrow \frac{1}{M} \sum_{m=1}^M w^{(m)}$.

B Method details

In this section, we present detailed descriptions of the score estimation strategies, resampling schemes, and numerical techniques used to improve our method. We also discuss the associated computational complexity.

B.1 Score estimation

In this subsection, we present several score estimators, including IS, AIS and SMC. AIS and SMC can be used to improve score estimates for complex targets.

B.1.1 IS-based score estimator

The IS-based estimator is summarized in Algorithm 2. Specifically, we relate the score function to the posterior mean via Tweedie's formula [44]:

$$\nabla_{x_t} \log p(x_t) = \frac{\alpha_t \mathbb{E}[\mathbf{u}_t \mid x_t] - x_t}{\sigma_t^2}.$$

This connection reduces the problem of estimating the score function to estimating the posterior mean $\mathbb{E}[\mathbf{u}_t \mid x_t]$. Importance sampling is used to approximate the posterior distribution. We sample from a proposal distribution q and reweight the samples \mathbf{u}_t according to their likelihood under the intermediate target distributions. We also derive the marginal estimate as a byproduct.

B.1.2 AIS and SMC-based score estimator

Algorithm 3 details an AIS-based approach [24] to construct the score estimate and marginal estimate.

AIS introduces a sequence of intermediate unnormalized distributions, smoothly bridging a tractable initial proposal distribution $q(x_0 \mid x_t)$ to the posterior distribution of interest $p(x_0 \mid x_t) \propto \tilde{\pi}(u) \mathcal{N}(x_t \mid \alpha_t u, \sigma_t^2 \mathbb{I})$. Algorithm 3 uses a geometric annealing schedule, setting intermediate targets $\nu_k(x_0) \propto q(x_0 \mid x_t)^{1-\beta_k} p(x_0 \mid x_t)^{\beta_k}$ where $\beta_k = k/n_{\text{steps}}$ for $k = 0, \dots, n_{\text{steps}}$.

Algorithm 3 begins by drawing a set of particles from the proposal distribution $q(x_0 \mid x_t)$. Then it gradually transitions these particles by running MCMC with a kernel invariant to the intermediate targets $\nu_k(x_0)$ for $k = 0, \dots, n_{\text{steps}} - 1$. In this work we mainly consider Hamiltonian Monte Carlo [HMC, 45] and Langevin Dynamics [LG, 46]. At each intermediate step, the algorithm updates the importance weights of each particle based on the ratio of successive intermediate targets.

The final weighted set of particles provides a consistent estimate of the desired posterior, which is utilized to construct a score estimate $s(x_t, \mathbf{u}_t)$, where \mathbf{u}_t denotes all the randomness in this procedure. Additionally, these weights provide an unbiased estimate of the unnormalized constant $\hat{p}(x_t, \mathbf{u}_t)$.

Notably, if we resample particles based on the weights at each intermediate step, the AIS procedure effectively becomes an SMC algorithm. In that case, the incremental weight is set to $w_k^{(m)} \leftarrow \frac{\nu_{k+1}(u^{(k,m)})}{\nu_k(u^{(k,m)})}$ for $k = 0, \dots, n_{\text{steps}} - 1$ and $m = 1, \dots, n_{\text{is}}$, and the marginal estimate becomes $\hat{p}(x_t, \mathbf{u}_t) \leftarrow \frac{1}{n_{\text{steps}}} \sum_{k=0}^{n_{\text{steps}}-1} \frac{1}{n_{\text{is}}} \sum_{m=1}^{n_{\text{is}}} w_k^{(m)}$. The other aspect of Algorithm 3 remains the same.

Algorithm 3: Annealed Importance Sampler of $p(x_0 \mid x_t) \propto \tilde{\pi}(x_0) \mathcal{N}(x_t \mid \alpha_t x_0, \sigma_t^2 \mathbb{I})$

Input: Unnormalized prior $\tilde{\pi}(\cdot)$, likelihood parameters $\{\alpha_t, \sigma_t\}$, data x_t , annealing schedule $0 = \beta_0 < \beta_1 < \dots < \beta_{n_{\text{steps}}} = 1$, number of importance samples n_{is} , initial proposal distribution $q(\cdot \mid x_t)$, MCMC transition kernel \mathcal{T} , MCMC steps per transition m_{steps} , and step size δ_{mcmc} .

Output: Score estimate $s(x_t, \underline{u}_t)$ and marginal estimate $\hat{p}(x_t, \underline{u}_t)$

- 1 Set annealing schedule $\beta_k \leftarrow k/n_{\text{steps}}$ for $k = 0, \dots, n_{\text{steps}}$;
- 2 Set initial target: $\nu_1(u) \propto q(u \mid x_t)^{1-\beta_1} \tilde{\pi}(u)^{\beta_1} \mathcal{N}(x_t \mid \alpha_t u, \sigma_t^2 \mathbb{I})^{\beta_1}$;
- 3 **for** $m \leftarrow 1$ **to** n_{is} **do**
 - 4 Sample initial particle $u^{(0,m)} \sim q(u \mid x_t)$;
 - 5 Initialize weight $w^{(m)} \leftarrow \frac{\nu_1(u^{(0,m)})}{q(u^{(0,m)} \mid x_t)}$;
- 6 **for** $k \leftarrow 1$ **to** $n_{\text{steps}} - 1$ **do**
 - 7 Set next target: $\nu_{k+1}(u) \propto q(u \mid x_t)^{1-\beta_{k+1}} \tilde{\pi}(u)^{\beta_{k+1}} \mathcal{N}(x_t \mid \alpha_t u, \sigma_t^2 \mathbb{I})^{\beta_{k+1}}$;
 - 8 **for** $m \leftarrow 1$ **to** n_{is} **do**
 - 9 Apply MCMC transition with kernel \mathcal{T} for m_{steps} steps and step size δ_{mcmc} targeting $\nu_k(u)$ to obtain the final sample $u^{(k,m)}$ and denote the intermediate samples $\tilde{u}^{(k,m)}$;
 - 10 Update weight: $w^{(m)} \leftarrow w^{(m)} \frac{\nu_{k+1}(u^{(k,m)})}{\nu_k(u^{(k,m)})}$;
- 11 Denote auxiliary variable $\underline{u}_t \leftarrow \{u^{(0,m)}\} \cup \{u^{(k,m)}, \tilde{u}^{(k,m)}\}_{k=1}^{n_{\text{steps}}-1}$;
- 12 Compute normalized weights: $\tilde{w}^{(m)} = \frac{w^{(m)}}{\sum_{m'=1}^{n_{\text{is}}} w^{(m')}}$;
- 13 Compute score estimate: $s(x_t, \underline{u}_t) \leftarrow \sum_{m=1}^{n_{\text{is}}} \tilde{w}^{(m)} \frac{\alpha_t u^{(n_{\text{steps}}-1,m)} - x_t}{\sigma_t^2}$;
- 14 Compute marginal density estimate: $\hat{p}(x_t, \underline{u}_t) \leftarrow \frac{1}{n_{\text{is}}} \sum_{m=1}^{n_{\text{is}}} w^{(m)}$;

B.1.3 Proposal choices in IS/AIS-based score estimators.

Algorithm 2 and Algorithm 3 require specifying an (initial) proposal distribution $q(x_0 \mid x_t)$. The choice of proposal is flexible and should ideally approximate the true posterior $p(x_0 \mid x_t)$; the closer it is, the more effective the resulting estimator.

In the example given in the main paper, we consider a proposal based on the backward transition kernel (i.e., the likelihood), which has also been used in prior work [8, 11, 43]. This proposal is effective when the likelihood signal is strong—i.e., when t is close to 0—but becomes less efficient as t increases and the signal weakens.

Alternative strategies include using a Gaussian proposal centered at the current x_t . If additional information about the target distribution is available—such as its mean or covariance—it can be incorporated into the proposal. For instance, one may use a Laplace approximation of the target to construct an approximate posterior, which can be used as a sensible proposal.

B.2 Score estimator based on other score identities

In Eq. (5) of the main paper, we derive the score estimator based on DSI in Eq. (3). Alternative score estimators can be derived based on other expressions of the score.

Based on TSI in Eq. (17), we obtain another estimate:

$$\nabla_{x_t} \log p(x_t) \approx s(x_t, \underline{u}_t) := \sum_{m=1}^M \frac{w^{(m)}}{\sum_{m'=1}^M w^{(m')}} \cdot \frac{\nabla_{\underline{u}_t} \log q(\underline{u}_t^{(m)})}{\alpha_t}, \quad (19)$$

where $\{w^{(m)}, \underline{u}_t^{(m)}\}_{m=1}^M$ is a weighted system approximating the posterior $p(x_0 \mid x_t)$ using an IS/AIS/SMC procedure.

Or, given MSI in Eq. (18), we have:

$$\nabla_{x_t} \log p(x_t) \approx s(x_t, \underline{u}_t) := \sum_{m=1}^M \frac{w^{(m)}}{\sum_{m'=1}^M w^{(m')}} \cdot \left(\alpha_t(\underline{u}_t^{(m)}) + \nabla_{\underline{u}_t} \log q(\underline{u}_t^{(m)}) \right) - x_t. \quad (20)$$

We primarily consider DSI and TSI-based estimators in our experiments.

B.3 SMC resampling and score clipping

We discuss two strategies to reduce the variance introduced by SMC resampling steps, and to address the potential high variance of score estimates, respectively.

SMC resampling strategy. While the resampling step in RDSMC is crucial for steering particles toward high target probability region, it introduces extra variance in the short term. We discuss several strategies to reduce this added variance.

We use systematic resampling, which introduces correlations among resampling indices [22, Chapter 2.2.1].

We also consider start resampling at a later stage of the sampling trajectory. At early steps, the Gaussian likelihood provides weaker conditional information, making posterior inference more challenging [8, 9]. Consequently, both the score estimates and marginal density estimates can be significantly biased or exhibit high variance, especially under limited compute budgets. As a result, the intermediate target distributions in early steps may not be sufficiently informative to enable effective resampling. To mitigate this issue, we delay resampling until a designated step $t_{\text{start-resampling}} < T$, which we treat as a tunable hyperparameter. In our experiments, we found that values in the range of $[0.3T, 0.8T]$ yielded improved performance.

After this point, we adopt an effective sample size (ESS)-based criterion to decide whether resampling should be performed at each step – a common strategy in SMC literature [22, Chapter 2.2.2]. The ESS at step t is computed as

$$ESS_t := \frac{\left(\sum_{i=1}^N w_t^{(i)} \right)^2}{\sum_{i=1}^N \left(w_t^{(i)} \right)^2}. \quad (21)$$

We trigger resampling only when the normalized ESS, computed as ESS_t/N , is below a threshold κ_{ess} , another hyperparameter which we fix at 0.3 throughout experiments.

When resampling is skipped (i.e. for $t > t_{\text{start-resampling}}$ or when the normalized ESS is above κ_{ess}), we must adjust the computation of the intermediate weights to ensure the unbiasedness of the log normalization constant estimate [22, Chapter 2.2.3]. For iterations where resampling is not performed, the weight update in Line 13 of Algorithm 1 is replaced by

$$w_t^{(i)} \leftarrow \frac{\bar{w}_{t+1}^{(i)}}{1/N} \cdot \frac{\hat{p}_t^{(i)} p(x_{t+1}^{(i)} | x_t^{(i)})}{\hat{p}_{t+1}^{(i)} q(x_t^{(i)} | x_{t+1}^{(i)}, \underline{u}_{t+1}^{(i)})} \quad (22)$$

where $\{\bar{w}_{t+1}^{(i)}\}_{i=1}^N$ are the normalized weights in the previous iteration.

Score clipping. To improve numerical stability, one may consider clipping the score estimates within a pre-specified range. As observed in prior work [47], score estimates produced by the TSI estimator defined in Eq. (17) can exhibit high variance or have large magnitudes, especially during early steps. Akhoun-Sadegh et al. [11] apply score norm clipping when training diffusion-based neural samplers with a loss of TSI-based score matching. Inspired by their work, we also clip the norm of the score estimates to a maximum of 20 when we use TSI estimate in the experiments. In contrast, we do not apply clipping when using the DSI-based score estimator.

B.4 Computational complexity

The total computational cost of RDSMC scales linearly with the number of diffusion discretization steps T , the number of particles N , and the cost of each score estimation step, denoted by M .

Specifically, for AIS-based score estimator as described in Algorithm 3, the cost M scales linearly with the number of importance samples n_{is} , the number of AIS transition steps n_{steps} , and the number of MCMC steps per transition m_{steps} . The vanilla IS-based score estimator in Algorithm 2 is a special case with $n_{\text{steps}} = 1$ and $m_{\text{steps}} = 1$.

Among these factors, the operations involving T , n_{steps} , and m_{steps} must be processed sequentially due to their time-dependent structure. In contrast, computations over the particles N and the importance samples n_{is} are embarrassingly parallel and can be efficiently distributed across parallel compute resources.

C Theoretical guarantees of RDSMC

We formally state the theorem providing sufficient conditions for asymptotic accuracy of RDSMC and unbiasedness of the estimate of the normalization constant. Our proof strategy for asymptotic accuracy is adapted from Wu et al. [30] and the proof for unbiasedness follows the techniques presented in Naesseth et al. [22].

Theorem 2. *Assume*

- (a) *the first marginal estimate $\hat{p}(x_T, \mathbf{u}_T)$, and the ratios of subsequent ratio $\hat{p}(x_t, \mathbf{u}_t)/\hat{p}(x_{t+1}, \mathbf{u}_{t+1})$ are positive and bounded,*
- (b) *the score estimate $s(x_t, \mathbf{u}_t)$ is bounded, and x_t has compact support,*
- (c) *variance increases in the forward noising kernel, i.e. for each t , $g_{t+1}^2 > g_t^2$.*

Then the RDSMC algorithm described in Algorithm 1 provides a consistent estimator of the target distribution $\pi(x_0)$ as particle size $N \rightarrow \infty$ and an unbiased estimator of the normalization constant Z for any $N \geq 1$. More specifically,

- (a) *Let $\mathbb{P}_N = \sum_{i=1}^N w_0^{(i)} \delta_{x_0^{(i)}}$ for weighted particles $\{(x_0^{(i)}, w_0^{(i)})\}_{i=1}^N$ returned by Algorithm 1 with N particles. \mathbb{P}_N converges setwise to $\pi(x_0)$ with probability one, that is for every set A , $\lim_{N \rightarrow \infty} \mathbb{P}_N(A) = \int_A \pi(x_0) dx_0$.*

- (b) *For the estimate for the normalization constant \hat{Z} returned by Algorithm 1, we have $\mathbb{E} \hat{Z} = Z$.*

The assumptions of Theorem 2 are typically satisfied in standard implementations of SMC samplers:

- Assumption (a) can be satisfied by the clipping of the marginal estimates $\hat{p}(x_t, \mathbf{u}_t)$ within the range $[c, C]$ for some constants $c, C > 0$.
- Assumption (b) by clipping scores estimates as well. Additionally, the compactness of the state space x_t is a standard and commonly adopted assumption in the SMC literature.
- Assumption (c) is mild and typically satisfied in practice. In both VE and VP noising schedules commonly used in diffusion models, the variance of the forward kernel increases with time.

Proof of Theorem 2: We first prove the asymptotic exactness of our sampler and then prove the unbiasedness of the normalization constant estimate.

First, Theorem 3 characterizes a set of conditions under which SMC algorithms converge. We restate this result below in our own notation.

Theorem 3 (Chopin and Papaspiliopoulos [19] – Proposition 11.4). *Let $\{(x_0^{(i)}, w_0^{(i)})\}_{i=1}^N$ be the particles and weights returned at the last iteration of a sequential Monte Carlo algorithm with N particles using multinomial resampling. If each weighting function w_t is positive and bounded, then for every bounded, ν_0 - measurable function ϕ of x_t*

$$\lim_{N \rightarrow \infty} \sum_{i=1}^N w_0^{(i)} \phi(x_0^{(i)}) = \int \phi(x_0) \nu_0(x_0) dx_0.$$

with probability one.

An immediate consequence of Theorem 3 is the setwise convergence of the discrete measures. To apply Theorem 3 to show asymptotic accuracy, it is sufficient to show that the weights at each step are upper bounded, as they are defined through probabilities and hence are positive. Since there is a finite number of steps T , it suffices to show that each w_t is bounded.

The initial weight is defined by

$$w_T = \frac{\hat{p}(x_T, \mathbf{u}_t)}{p(x_T)},$$

which is bounded by Assumption (a).

The intermediate weights are defined by Eq. (14) such that

$$w_t = \frac{\hat{p}(x_t, \mathbf{u}_t) p(x_{t+1} | x_t)}{\hat{p}(x_{t+1}, \mathbf{u}_{t+1}) q(x_t | x_{t+1}, \mathbf{u}_{t+1})}.$$

We first decompose the weights by

$$\log w_t = \log \frac{\hat{p}(x_t, \mathbf{u}_t)}{\hat{p}(x_{t+1}, \mathbf{u}_{t+1})} + \log \frac{p(x_{t+1} | x_t)}{q(x_t | x_{t+1}, \mathbf{u}_{t+1})}.$$

The boundedness of $\log \frac{\hat{p}(x_t, \mathbf{u}_t)}{\hat{p}(x_{t+1}, \mathbf{u}_{t+1})}$ is guaranteed by Assumption (a). We now show the boundedness of $\log \frac{p(x_{t+1} | x_t)}{q(x_t | x_{t+1}, \mathbf{u}_{t+1})}$. First, note that

$$p(x_{t+1} | x_t) = \mathcal{N}(x_{t+1} | x_t + f_t x_t \delta, g_t^2 \delta),$$

and

$$q(x_t | x_{t+1}, \mathbf{u}_{t+1}) = \mathcal{N}(x_t | x_{t+1} - [f_{t+1} x_{t+1} - g_{t+1}^2 s(x_{t+1}, \mathbf{u}_{t+1})] \delta, g_{t+1}^2 \delta).$$

Let $\hat{\mu}_p = x_{t+1} - f_t x_t \delta$ and $\hat{\mu}_q = x_{t+1} - [f_{t+1} x_{t+1} - g_{t+1}^2 s(x_{t+1}, \mathbf{u}_{t+1})] \delta$. We can show that $\|\hat{\mu}_p - \hat{\mu}_q\| = \|f_{t+1} x_{t+1} - f_t x_t - g_{t+1}^2 s(x_{t+1}, \mathbf{u}_{t+1})\| \delta$ is bounded, which follows from Assumption (b). The log-ratio then simplifies as

$$\log \frac{p(x_{t+1} | x_t)}{q(x_t | x_{t+1}, \mathbf{u}_{t+1})} \tag{23}$$

$$= \log \frac{|2\pi g_t^2 I|^{-1/2} \exp\{-(2g_t^2)^{-1} \|x_t - \hat{\mu}_p\|^2\}}{|2\pi g_{t+1}^2 I|^{-1/2} \exp\{-(2g_{t+1}^2)^{-1} \|x_t - \hat{\mu}_q\|^2\}} \tag{24}$$

$$\text{Rearrange and let } C = \log |2\pi g_t^2 I|^{-1/2} / |2\pi g_{t+1}^2 I|^{-1/2} \tag{25}$$

$$= -\frac{1}{2} [g_t^{-2} \|x_t - \hat{\mu}_p\|^2 - g_{t+1}^{-2} \|x_t - \hat{\mu}_q\|^2] + C \tag{26}$$

$$\text{Expand and rearrange } \|x_t - \hat{\mu}_q\|^2 = \|x_t - \hat{\mu}_p\|^2 + 2\langle \hat{\mu}_p - \hat{\mu}_q, x_t - \hat{\mu}_p \rangle + \|\hat{\mu}_p - \hat{\mu}_q\|^2 \tag{27}$$

$$= -\frac{1}{2} [(g_t^{-2} - g_{t+1}^{-2}) \|x_t - \hat{\mu}_p\|^2 - 2g_{t+1}^{-2} \langle \hat{\mu}_p - \hat{\mu}_q, x_t - \hat{\mu}_p \rangle - g_{t+1}^{-2} \|\hat{\mu}_p - \hat{\mu}_q\|^2] + C \tag{28}$$

$$\text{Let } C' = C + \frac{1}{2} g_{t+1}^2 \|\hat{\mu}_p - \hat{\mu}_q\|^2 \text{ and rearrange. Note that } \|\hat{\mu}_p - \hat{\mu}_q\|^2 < \infty \tag{29}$$

$$= -\frac{1}{2} (g_t^{-2} - g_{t+1}^{-2}) \|x_t - \hat{\mu}_p\|^2 + g_{t+1}^{-2} \langle \hat{\mu}_p - \hat{\mu}_q, x_t - \hat{\mu}_p \rangle + C' \tag{30}$$

$$\text{By Cauchy-Schwarz,} \tag{31}$$

$$\leq -\frac{1}{2} (g_t^{-2} - g_{t+1}^{-2}) \|x_t - \hat{\mu}_p\|^2 + g_{t+1}^{-2} \|\hat{\mu}_p - \hat{\mu}_q\| \cdot \|x_t - \hat{\mu}_p\| + C' \tag{32}$$

$$\text{By Assumption (c), } g_t^{-2} - g_{t+1}^{-2} > 0, \tag{33}$$

$$\leq \frac{1}{2} \frac{(g_{t+1}^{-2} \|\hat{\mu}_p - \hat{\mu}_q\|)^2}{g_t^{-2} - g_{t+1}^{-2}} + C' \tag{34}$$

$$= \frac{g_{t+1}^{-4}}{2(g_t^{-2} - g_{t+1}^{-2})} \|\hat{\mu}_p - \hat{\mu}_q\|^2 + C' \tag{35}$$

$$\leq C''. \tag{36}$$

The final line follows from the boundedness of $\|\hat{\mu}_p - \hat{\mu}_q\|$. The above derivation shows that each w_t is bounded, which concludes the proof for the asymptotic exactness of our sampler.

Then we show the unbiasedness of the normalization constant estimate \hat{Z} . Let a_t^i be the index of $x_t^{(i)}$ and $u_t^{(i)}$ before resampling. With that, \hat{Z} is defined by

$$\hat{Z} = \prod_{t=0}^T \frac{1}{N} \sum_{i=1}^N w_t^{(i)}, \quad \text{where } w_t^{(i)} = \frac{\hat{p}_t^{(i)} p(x_{t+1}^{(i)} | x_t^{a_t^i})}{\hat{p}_{t+1}^{(i)} q(x_t^{a_t^i} | x_{t+1}^{(i)}, u_{t+1}^{(i)})}, \quad w_T^{(i)} = \frac{\hat{p}_T^{(i)}}{\hat{p}(x_T^{a_t^i})}.$$

Denote the normalized weight by $\tilde{w}_t^{(i)} = \frac{w_t^{(i)}}{\sum_{i=1}^N w_t^{(i)}}$. The distribution of all random variables generated by the SMC method is then given by

$$\begin{aligned} & Q(x_{0:T}, u_{0:T}, a_{0:T}) \\ &= p(x_T, u_T) p(x_{0:T-1}, u_{0:T-1}, a_{0:T}) \\ &= p(x_T^{a_T}, u_T^{a_T}) p(x_T, u_T | x_T^{a_T}, u_T^{a_T}) \prod_{t=0}^{T-1} p(x_t, u_t | x_t^{a_t}, u_t^{a_t}) q(x_t^{a_t} | x_{t+1}, u_{t+1}) q(u_t^{a_t} | x_t^{a_t}), \\ &= p(x_T^{a_T}) \left(\prod_{i=1}^N \frac{w_T^{(i)}}{\sum_{i=1}^N w_T^{(i)}} \right) \prod_{i=1}^N \left[\left(\prod_{t=0}^{T-1} \frac{w_t^{(i)}}{\sum_{i=1}^N w_t^{(i)}} q(x_t^{a_t^i} | x_{t+1}^{(i)}, u_{t+1}^{(i)}) \right) \right] \\ & \quad \left[q(u_T^{a_T} | x_T^{a_T}) \prod_{t=0}^{T-1} q(u_t^{a_t} | x_t^{a_t}) \right]. \end{aligned}$$

By $w_t^{(i)} = \frac{\hat{p}_t^{(i)} p(x_{t+1}^{(i)} | x_t^{a_t^i})}{\hat{p}_{t+1}^{(i)} q(x_t^{a_t^i} | x_{t+1}^{(i)}, u_{t+1}^{(i)})}$ and $w_T^{(i)} = \frac{\hat{p}_T^{(i)}}{p(x_T^{a_T})}$, we have:

$$\begin{aligned} & Q(x_{0:T}, u_{0:T}, a_{0:T}) \\ &= \left(\prod_{t=0}^T \sum_{i=1}^N w_t^{(i)} \right)^{-1} \hat{p}_0^{(1)} \left(\prod_{t=0}^{T-1} p(x_{t+1}^{(1)} | x_t^{a_t^1}) \right) \\ & \quad \prod_{i=2}^N \hat{p}_T^{(i)} \prod_{i=2}^N \left[\left(\prod_{t=0}^{T-1} \tilde{w}_t^{(i)} q(x_t^{a_t^i} | x_{t+1}^{(i)}, u_{t+1}^{(i)}) \right) \right] \left[q(u_T^{a_T} | x_T^{a_T}) \prod_{t=0}^{T-1} q(u_t^{a_t} | x_t^{a_t}) \right], \end{aligned}$$

where we plug in $w_t^{(1)}$ and rearrange terms.

By multiplying \hat{Z} , we have:

$$\begin{aligned} \hat{Z} Q(x_{0:T}, u_{0:T}, a_{0:T}) &= \hat{Z} \left(\prod_{t=0}^T \sum_{i=1}^N w_t^{(i)} \right)^{-1} \hat{p}_0^{(1)} \left(\prod_{t=0}^{T-1} p(x_{t+1}^{(1)} | x_t^{a_t^1}) \right) \\ & \quad \prod_{i=2}^N \left[\hat{p}_T^{(i)} \left(\prod_{t=0}^{T-1} \tilde{w}_t^{(i)} q(x_t^{a_t^i} | x_{t+1}^{(i)}, u_{t+1}^{(i)}) \right) \right] \left[q(u_T^{a_T} | x_T^{a_T}) \prod_{t=0}^{T-1} q(u_t^{a_t} | x_t^{a_t}) \right] \\ &= N^{-T} \hat{p}_0^{(1)} q(u_0^{a_0^1} | x_0^{a_0^1}) \left(\prod_{t=0}^{T-1} p(x_{t+1}^{(1)} | x_t^{a_t^1}) q(u_{t+1}^{a_{t+1}^1} | x_{t+1}^{a_{t+1}^1}) \right) \\ & \quad \prod_{i=2}^N \left[\hat{p}_T^{(i)} q(u_t^{a_t^i} | x_t^{a_t^i}) \left(\prod_{t=0}^{T-1} \tilde{w}_t^{(i)} q(x_t^{a_t^i} | x_{t+1}^{(i)}, u_{t+1}^{(i)}) q(u_{t+1}^{a_{t+1}^i} | x_{t+1}^{a_{t+1}^i}) \right) \right], \end{aligned}$$

where the first equality follows from plugging in Q and the second follows from plugging in \hat{Z} .

The expectation of the normalization constant estimate can be written as

$$\begin{aligned}
\mathbb{E}_Q(\hat{Z}) &= N^{-T} \sum_{a_{0:T}} \int \int \hat{p}_0^{(1)} q(u_0^{a_0^1} | x_0^{a_0^1}) \left(\prod_{t=0}^{T-1} p(x_{t+1}^{(1)} | x_t^{a_t^1}) q(\underline{u}_{t+1}^{a_{t+1}^1} | x_{t+1}^{a_{t+1}^1}) \right) \\
&\quad \prod_{i=2}^N \left[\hat{p}_T^{(i)} q(u_t^{a_T^i} | x_t^{a_T^i}) \left(\prod_{t=0}^{T-1} \widetilde{w}_t^{(i)} q(x_t^{a_t^i} | x_{t+1}^{(i)}, \underline{u}_{t+1}^{(i)}) q(\underline{u}_{t+1}^{a_{t+1}^{(i)}} | x_{t+1}^{a_{t+1}^{(i)}}) \right) \right] dx_{0:T} du_{0:T} \\
&= N^{-T} \sum_{a_{0:T}} \int \int \hat{p}_0^{(1)} q(u_0^{a_0^1} | x_0^{a_0^1}) \left(\prod_{t=0}^{T-1} p(x_{t+1}^{(1)} | x_t^{a_t^1}) q(\underline{u}_{t+1}^{a_{t+1}^1} | x_{t+1}^{a_{t+1}^1}) \right) dx_{0:T}^1 du_{0:T}^1 \\
&= Z,
\end{aligned}$$

where in the second equality, we marginalize the variables not involved in the particle $x_{0:T}^1$ and $x_{0:T}^{a_{0:T}^1}$. The final equality follows because we are averaging over N^T possible cases of $a_{0:T}^1$ and all are equal to Z , which concludes the proof.

D Experiment details

This section provides additional experiment details. Appendix D.1 describes the implementation and hyperparameter details of RDSMC and all competing baselines. Appendices D.2 to D.4 include supplementary information and additional results for different targets in the main experiments.

Compute resources. All experiments were conducted on a single NVIDIA A100 GPU with 40 GB GPU memory, and accessed between 16 GB and 32 GB of CPU memory, depending on the task.

D.1 Method and hyperparameter details

We first give an overview of baseline methods we benchmark RDSMC against. We then describe key hyperparameter settings of our method and competing baselines.

D.1.1 Summary of baseline methods

AIS [24]. The annealed importance sampling (AIS) algorithm defines a sequence of geometrically annealed distributions $\rho_t(x)$ for $t \in \{0, 1, \dots, T\}$ from an initial proposal $\rho_0(x)$ to the desired target $\rho_T(x) \propto \pi(x)$ as $\rho_t(x) \propto \rho_0(x)^{1-\beta_t} \pi(x)^{\beta_t}$ where $\{\beta_t\}_{t=0}^T$ is an increasing linear schedule with $\beta_t = t/T$. AIS begins by sampling from the initial proposal $\rho_0(x)$ and proceeds through a sequence of MCMC transitions, each targeting the intermediate distribution $\rho_t(x)$. The resulting weighted samples provide a consistent approximation to the target distribution $\pi(x)$.

SMC [25]. Sequential Monte Carlo (SMC) operates on the same sequence of annealed distributions as AIS but differs by performing resampling at certain iterations. In our implementation, we consider both constant resampling at each step and an adaptive strategy based on an ESS threshold κ_{ess} .

RDMC [8] Reverse diffusion Monte Carlo (RDMC) builds on the time-reversed Ornstein–Uhlenbeck diffusion:

$$dY_t = \{Y_t + 2 \nabla \log p_{t_{\text{init}}-t}(Y_t)\} dt + \sqrt{2} dB_t, \quad Y_0 \sim p_{t_{\text{init}}}$$

where $p_s(y) = \int \mathcal{N}(y; e^{-s}x, (1 - e^{-2s})I) \pi(dx)$. By Tweedie’s formula, the intractable score $\nabla \log p_{t_{\text{init}}-t}(Y_t)$ can be written in terms of the posterior denoiser:

$$u_t(y) = \int x q_t(x | y) dx, \quad q_t(x | y) \propto \pi(x) \mathcal{N}(x; e^{t_{\text{init}}-t}y, (e^{2(t_{\text{init}}-t)} - 1)I),$$

so that the SDE becomes

$$dY_t = \left\{ \frac{e^{-2(t_{\text{init}}-t)}+1}{e^{-2(t_{\text{init}}-t)}-1} Y_t + \frac{2e^{-(t_{\text{init}}-t)}}{1-e^{-2(t_{\text{init}}-t)}} u_t(Y_t) \right\} dt + \sqrt{2} dB_t.$$

Following the implementation of Grenioux et al. [9], RDMC discretizes the interval $[0, t_{\text{init}}]$ into T steps. At initialization, RDMC employs a *Langevin-within-Langevin* scheme to sample from $p_{t_{\text{init}}}$: using Unadjusted Langevin Algorithm (ULA) where the score function is estimated based on DSI. In subsequent steps, RDMC simulates from the reverse SDE where the denoiser $u_t(y)$ is obtained by running the Metropolis-adjusted Langevin Algorithm (MALA) targeting $q_t(x | y)$.

SLIPS [9] Stochastic Localization via Iterative Posterior Sampling (SLIPS) relies on a stochastic observation process defined as:

$$Y_t = \alpha(t)X + \sigma W_t,$$

where $(W_t)_{t \geq 0}$ is a standard Brownian motion independent of $X \sim \pi$, and $\alpha(t)$ is a flexible denoising schedule function. To bypass the direct sampling requirement from π , SLIPS introduces a conditional denoiser defined by:

$$u_t(y) = \int x q_t(x | y) dx, \quad q_t(x | y) \propto \pi(x) \mathcal{N}\left(\frac{y}{\alpha(t)}, \frac{\sigma^2}{g(t)^2} I\right).$$

The corresponding SDE governing this observation process is:

$$dY_t = \dot{\alpha}(t)u_t(Y_t)dt + \sigma dB_t, \quad (37)$$

where $(B_t)_{t \geq 0}$ is another standard Brownian motion.

Similar to RDMC, the SLIPS algorithm approximates the dynamics defined by this SDE using an MCMC approach to estimate the conditional denoiser u_t or a related score function:

- The SLIPS initialization also involves a *Langevin-within-Langevin* procedure. Different from RDMC, SLIPS chooses the initialization time t_{init} such that both the marginal $p_{t_{\text{init}}}(y)$ and the posterior $q_{t_{\text{init}}}(x | y)$ are (approximately) log-concave, which they refer to as the “duality of log-concavity” assumption.
- In the subsequent steps, SLIPS integrates the observation process where the denoiser $u_t(Y_t)$ is estimated by MALA sampling from $q_t(x | y)$.

SMS [33]. For a target π , Sequential Multimeasurement Sampler (SMS) draws M independent noisy observations at some noise scale $\sigma > 0$:

$$Y^m = X + \sigma Z^m, \quad Z^m \sim \mathcal{N}(0, I), \quad m = 1, \dots, M,$$

with $X \sim \pi$. For any $m \in \{1, \dots, M\}$, the posterior density of X given $y_{1:m}$ is

$$q_m(x | y_{1:m}) \propto \pi(x) \mathcal{N}(\bar{y}_{1:m}, \frac{\sigma^2}{m} I),$$

where $\bar{y}_{1:m} = (1/m) \sum_{i=1}^m y_i$. Its Bayes estimator

$$u_m(y_{1:m}) = \mathbb{E}[X | Y^{1:m} = y_{1:m}]$$

serves as a non-Markovian denoiser, and one shows that the law of $u_m(Y^{1:m})$ converges to π in W_2 at rate $O(\sigma \sqrt{d/m})$ [33].

To sample from π , one first simulates the entire M -tuple $Y^{1:M}$ and then returns $u_M(Y^{1:M})$. They employ a ‘Once-At-A-Time’ strategy: draw Y^1 (whose marginal is $\pi \mathcal{N}(0, \sigma^2 I)$) via Underdamped Langevin, then sequentially sample each $Y^m | Y^{1:m-1}$ using MCMC targeting the conditional density of Y^m . Under mild assumptions this sequence of targets becomes increasingly log-concave in m , but the initial draw of Y^1 can be as challenging as sampling from π itself when σ is large. Although one can estimate scores via importance sampling or inner-loop posterior MCMC, numerical results show a steep degradation in performance unless σ is carefully tuned—a manifestation of the same “duality of log-concavity” that forces a trade-off between ease of initialization and overall convergence as reported by Grenioux et al. [48].

D.1.2 Implementation details and hyperparameter settings

RDSMC. We summarize the hyperparameter values used to tune RDSMC and its variants in different experiments in Table 3. Key hyperparameters are explained below.

Target	n_{is}	n_{steps}	δ_{mcmc}	$t_{start-resampling}$	score est.	mcmc kernel
GMM ($d = 2, 4$)	{10, 100}	{1, 10}	{1.0}	{0.5, 0.8}	DSI	HMC
GMM ($d = 8 - 64$)	{10, 100}	{1, 10, 50}	{1.0}	{0.5, 0.8}	DSI	HMC
Rings	{100}	{1, 10}	{0.01, 0.05}	{0.5}	DSI	LG
Funnel	{100}	{1, 10, 50}	{0.01, 0.05}	{0.5, 0.8}	DSI	LG
Logistic Reg.	{10, 100}	{10, 50}	{0.01, 0.005}	{0.5, 0.8}	TSI	LG

Table 3: Hyperparameter grid used for tuning RDSMC. We fix the number of sampling steps at $T = 100$, set $m_{steps} = 1$ MCMC step per AIS transition, and use an ESS threshold of $\kappa_{ess} = 0.3$. Score estimator and MCMC kernel types are selected via a coarse grid search using validation metrics. RDSMC (IS) and RDSMC (Proposal) use the same grid with $\kappa_{ess} = 0$, excluding $t_{start-resampling}$ as it does apply in these settings.

We consider the VP diffusion schedule described in Eq. (16). We fix RDSMC to use $T = 100$ time discretization steps evenly spaced between $[0, 1]$. The remaining hyperparameters pertain to the MC score estimation and the SMC procedure.

For MC score estimation, we use AIS (Algorithm 3), with vanilla IS (Algorithm 2) as a special case when $n_{steps} = 1$ (in which case m_{steps} is not applicable). Associated hyperparameters include

- Score estimator type: DSI (Eq. (5)) or TSI (Eq. (19)).
- MCMC transition kernel: Langevin dynamics (LG) or Hamiltonian Monte Carlo (HMC).
- n_{is} : Number of importance samples used in Monte Carlo score estimation
- n_{steps} : Number of intermediate distributions (i.e., AIS steps).
- δ_{mcmc} : Step size used in the MCMC transition kernel.
- m_{steps} : Number of MCMC steps per AIS transition. We use $m_{steps} = 1$ in all experiments.

For SMC procedures related, we consider

- $t_{start-resampling}$: Starting step for resampling within the SMC trajectory. No resampling is performed for $t > t_{start-resampling}$.
- κ_{ess} : Normalized effective sample size threshold triggering resampling. When $\kappa_{ess} = 0$, no resampling is applied throughout; this corresponds to RDSMC (IS) when the final-step weighting is used, or RDSMC (Proposal) otherwise. We set $\kappa_{ess} = 0.3$ in all experiments involving RDSMC.

We select the score estimator and MCMC kernel types through a coarse grid search using validation metrics. And then we primarily tune n_{is} , n_{steps} , δ_{mcmc} and $t_{start-resampling}$, as described in Table 3.

The hyperparameter search grid for baseline methods is provided in Table 4. We largely follow the implementation of the official codebase of Grenioux et al. [9] (available at <https://github.com/h2o64/slips>). For the bi-modal GMM experiments, we tune key hyperparameters within a similar range to those used for RDSMC. For the Rings, Funnel, and Bayesian logistic regression tasks, we adopt the settings reported by Grenioux et al. [9].

We use the following target variance information to initialize AIS, SMC, and SLIPS. Crucially, RDMC and our method do not make use of this information.

We restate Assumption A0 from Grenioux et al. [9]

Assumption 1. *(Log-concavity outside a compact). There exist $R > 0$ and $\tau > 0$ such that π is the convolution of μ and $\mathcal{N}(0, \tau^2 \mathbf{I}_d)$, where μ is a distribution compactly supported on $\mathbb{B} = \mathbb{B}(\mathbf{m}_\pi, R)$, i.e., $\mu(\mathbb{R}^d \setminus \mathbb{B}) = 0$.*

The values of R and τ that approximately or exactly satisfy this assumption for different targets are provided in the corresponding experiment subsections.

We next discuss the hyperparameter settings for each of the baseline methods.

Target	AIS		SMC		SMS	
	$\delta_{\text{mcmc-init}}$	$\delta_{\text{mcmc-init}}$	κ_{ess}	δ_{mcmc}	δ_{γ}	
GMM	{0.1, 0.5, 1.0}	{0.1, 0.5, 1.0}	{0.3, 1.0}	{0.03, 1.0}	{0.0625, 0.05}	
Rings	{0.01}	{0.01}	{0.3, 1.0}	{0.03, 1.0}	{0.0625, 0.05}	
Funnel	{0.01}	{0.01}	{0.3, 1.0}	{0.03, 1.0}	{0.0625, 0.05}	
Logistic Reg.	{0.01}	{0.01}	{0.3, 1.0}	{0.03, 1.0}	{0.0625, 0.05}	

Target	RDMC		SLIPS	
	$\exp\{t_{\text{init}}\}$	t_{final}	ϵ	$\delta_{\text{mcmc-init}}$
GMM	{0.95, 0.9, 0.8, 0.7}	{150, 300}	{0.03, 0.05, 0.1, 0.2, 0.4}	{0.1, 0.5, 1.0}
Rings	{0.95, 0.9, 0.8, 0.7}	{150, 300}	{0.1, 0.2, 0.4, 1.0, 1.2}	{1e-5}
Funnel	{0.95, 0.9, 0.8, 0.7}	{150, 300}	{0.1, 0.2, 0.4, 1.0, 1.2}	{1e-5}
Logistic Reg.	{0.95, 0.9, 0.8, 0.7}	{150}	{0.03, 0.05, 0.1, 0.2, 0.4}	{1e-5}

Table 4: Hyperparameter grid used for tuning baseline methods. AIS, SMC, RDMC, and SLIPS use $T = 1,000$ sampling steps, and SMS uses $K = 500$ noisy observations. On GMM experiments, we add additional ablation for AIS and SMC with $T = 100$ steps.

AIS. AIS uses $T = 1,000$ annealing steps. Each transition step uses an MALA kernel with an adaptive step size, initialized at $\delta_{\text{mcmc-init}}$, to maintain the acceptance ratio at 75%. Additionally, MALA runs 4 parallel chains, each with 32 MCMC steps. The initial proposal $\rho_0(x)$ is set to $\mathcal{N}(x \mid 0, R^2 + \tau^2)$.

The only tunable parameter we consider is $\delta_{\text{mcmc-init}}$.

SMC. SMC follows the same configuration as AIS, except it incorporates ESS-based resampling, introducing the normalized ESS threshold κ_{ess} as an additional hyperparameter (alongside $\delta_{\text{mcmc-init}}$).

RDMC. RDMC uses $T = 1,000$ discretization steps. To initialize $p_{t_{\text{init}}}$ in RDMC, the Langevin-within-Langevin algorithm is simulated using 16 MCMC steps and 4 MCMC chains. The chains are initialized with an IS approximation of the posterior powered by 128 particles. The initial sample is drawn from $\mathcal{N}(0, (1 - \exp\{-2t_{\text{init}}\})\mathbb{I}_d)$ and the initial step size is set to $(1 - \exp\{-2t_{\text{init}}\})/2$.

Subsequent steps use a MALA kernel for posterior sampling with adaptive step size to maintain the acceptance ratio at 75%, 4 parallel chains and 32 MCMC steps. We drop the first 50 MCMC samples to ignore the warm-up period in the estimation.

The only tunable parameter we consider is t_{init} .

SLIPS. SLIPS follows a similar initialization and posterior sampling scheme as RDMC, also with $T = 1,000$ discretization steps. However, instead of tuning the value of the initial sampling time t_{init} , SLIPS makes use of the target variance information and sets $p_{t_{\text{init}}}(x) := \mathcal{N}(x \mid 0, R^2/d + \tau^2)$.

SLIPS also features a few algorithmic subtleties.

- SLIPS uses a stochastic exponential integrator scheme to simulate from their observational SDE, where ours and RDMC consider the Euler Maruyama scheme.
- SLIPS discretizes the SDE using evenly spaced points in the log-SNR space, while our method and RDMC perform discretization in the time domain.
- SLIPS reuses the final MCMC samples from the previous step as the initialization for MCMC at the next step, promoting continuity across iterations.
- At the final step, SLIPS outputs the estimated denoiser as an approximate sample from the target π to align with standard stochastic localization literature. In contrast, our method and RDMC return a random sample generated from the approximated SDE dynamics.

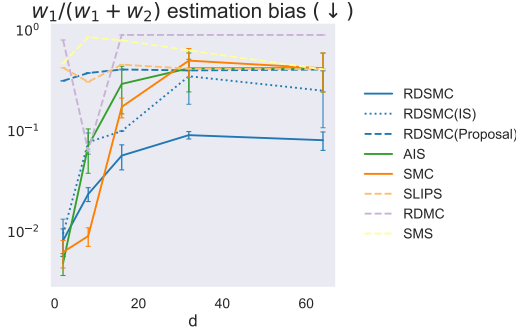


Figure 2: Estimation bias of weight ratio $w_1/(w_1 + w_2)$ versus dimension d . Results are averaged over 5 seeds with error bars showing one standard error. Bias increases with d for all methods, while RDSMC consistently outperforms the baselines.

We consider the following hyperparameters: (i) t_{final} the final integration time of Eq. (37), (ii) ϵ the initial time to determine the log-SNR-based discretization schedule, and (iii) $\delta_{\text{mcmc-init}}$, the initial step size for the MALA kernel.

SMS. We set the number of noisy observations M in SMS to $\lfloor T/2 \rfloor$ where $T = 1,000$, and use as many MCMC steps per noise level as SLIPS or RDMC. This choice of K ensures that the computational complexity of SMS is on par with other baseline methods. The Langevin steps are done using ULA as suggested by the authors.

We tune the step size δ_{mcmc} and the friction coefficient δ_γ using recommended values by the authors.

D.2 Bi-moddal gaussian mixtures

Target. We consider a Gaussian mixture model (GMM) with two components in a d -dimensional space. The component means m_1, m_2 are randomly initialized from a uniform distribution over a box of width 80, centered at the origin. Each component has diagonal covariance with all diagonal values equal to $\sigma^2 = 2 \log 2$. The weights are fixed to $[w_1, w_2] = [0.1, 0.9]$ regardless of dimension d . Formally, the target density is

$$\pi(x) = w_1 \mathcal{N}(x | m_1, \sigma^2 \mathbb{I}_d) + w_2 \mathcal{N}(x | m_2, \sigma^2 \mathbb{I}_d). \quad (38)$$

Metrics. We compute the estimated weights by assigning samples to different components.

For a sample x , we assign it to the component $k \in \{1, 2\}$ with highest posterior probability value, which is computed as

$$p(x \text{ in component } k) = \frac{w_k \mathcal{N}(x | \mu_k, \sigma^2 \mathbb{I}_d)}{\sum_{j=1}^2 w_j \mathcal{N}(x | \mu_j, \sigma^2 \mathbb{I}_d)}.$$

The weight estimates are then formulated as $\hat{w}_1 = \frac{1}{N} \sum_{i=1}^N \mathbf{1}\{x_i \text{ in component 1}\}$ and $\hat{w}_2 = 1 - \hat{w}_1$.

The weight estimation ratio bias is computed as $|\hat{w}_1/(\hat{w}_1 + \hat{w}_2) - w_1/(w_1 + w_2)| = |\hat{w}_1 - w_1|$.

The log normalization constant estimation bias is simply $|\hat{Z} - Z|$ where \hat{Z} is the estimated value, for method that computes it.

Additional implementation details. Assumption 1 are satisfied for $R = \max(w_1, w_2) \|m_1 - m_2\| = 0.9 \|m_1 - m_2\|$, and $\tau = \sigma$. These values are used to initialize AIS, SMC, SMS, and SLIPS.

For RDSMC and its variants, we use DSI to estimate the score. The initial proposal distribution in Algorithm 3 is set to $\mathcal{N}(x_0 | x_t/\alpha_t, \sigma_t^2/\alpha_t^2)$.

Additional results. Figure 1b in the main text displays the comparison among AIS, SMC, RDSMC and its variances for presentation clarity. Here, we present the full results of weight ratio estimation

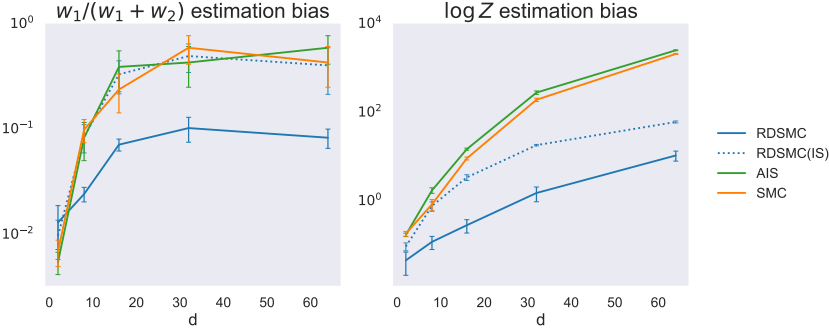


Figure 3: Estimation bias of weight ratio $w_1/(w_1 + w_2)$ and log normalization constant $\log Z$, with hyperparameters selected to minimize the $\log Z$ estimation bias. We observe that all methods exhibit monotonic trends in both bias metrics.

bias including SMS, RDMC, and SLIPS in Figure 2. We observe that SMS, RDMC, and SLIPS consistently underperform RDSMC across dimensions.

The hyperparameters used for results in Figures 1b and 2 are selected based on minimizing the estimation bias of weight ratio $w_1/(w_1 + w_2)$. Here, we also report results using hyperparameters tuned by minimizing the $\log Z$ bias in Figure 3. Results for RDSMC (Proposal), SMS, RDMC, and SLIPS are not included as they do not provide normalization constant estimate. The trends are largely similar, except that the $\log Z$ estimation bias curve appears monotonic.

D.3 Rings and Funnel distributions

Targets. The Rings distribution [9] is defined via an inverse polar reparameterization of a base distribution p_z , which is factorized into two independent univariate marginals p_r and p_θ :

- p_r is a mixture of four Gaussian distributions, each with mean located at integer radial positions $i + 1$ for $i \in \{0, 1, 2, 3\}$ and variance 0.15^2 .
- The angular component p_θ is uniformly distributed over $[0, 2\pi]$.

The Funnel distribution [34] is characterized by a hierarchical density structure in a 10-dimensional space, where the first dimension x_1 is drawn from a Gaussian distribution with zero mean and variance $\sigma^2 = 9$. The subsequent dimensions $x_{2:10}$ are conditionally Gaussian, with variances exponentially dependent on the first dimension. Formally, the density is

$$\pi(x_{1:10}) = \mathcal{N}(x_1; 0, \sigma^2) \mathcal{N}(x_{2:10}; 0, \exp(x_1) \mathbb{I}_9). \quad (39)$$

Metrics. The entropic regularized 2-Wasserstein distance between two distributions μ and ν is defined by

$$W_{2,\varepsilon}(\mu, \nu) = \inf \left\{ \int_{\mathbb{R}^d \times \mathbb{R}^d} \|x_1 - x_0\|^2 d\pi(x_0, x_1) - H(\pi) : \pi_0 = \mu, \pi_1 = \nu \right\}^{1/2}, \quad (40)$$

where $\varepsilon > 0$ is a regularization hyper-parameter and $H(\pi) = - \int_{\mathbb{R}^d \times \mathbb{R}^d} \log \pi(x_0, x_1) d\pi(x_0, x_1)$ refers to as the entropy of π . We evaluate the quality of sampling with regularization $\varepsilon = 0.05$ via POT library [49].

Total Variation Distance (TVD) measures the discrepancy between the true and model-generated distributions by comparing their marginal histograms within a bounded region.

Let $\hat{\mu}_i$ and $\hat{\nu}_i$ represent the probability mass in the i -th bin for the true and generated distributions, respectively. We compute the TVD as follows

$$\text{TVD} = \frac{1}{2} \sum_i |\hat{\mu}_i - \hat{\nu}_i|,$$

For the radius TVD, we generate the histogram of the radius samples using 256 uniform bins over the interval $[0, 8]$. For the angle TVD, we generate the histogram of angle samples using 256 uniform bins over the interval $[-\pi, \pi]$.

Algorithm	Sample W2	Radius TVD	Angle TVD	$\log Z$	Bias
AIS	0.19 ± 0.01	0.10 ± 0.00	0.15 ± 0.00	0.05 ± 0.00	
SMC	0.19 ± 0.01	0.10 ± 0.00	0.15 ± 0.00	0.05 ± 0.00	
SMS	0.23 ± 0.01	0.24 ± 0.01	0.14 ± 0.00		N/A
RDMC	0.41 ± 0.01	0.37 ± 0.00	0.14 ± 0.00		N/A
SLIPS	0.22 ± 0.01	0.19 ± 0.00	0.13 ± 0.00		N/A
RDSMC	0.26 ± 0.01	0.13 ± 0.01	0.21 ± 0.01	0.03 ± 0.00	
RDSMC(IS)	0.29 ± 0.01	0.15 ± 0.01	0.24 ± 0.00	0.02 ± 0.01	
RDSMC(Proposal)	0.18 ± 0.01	0.09 ± 0.00	0.14 ± 0.00		N/A

Table 5: Additional results for Rings. For all metrics, lower is better.

The Kolmogorov-Smirnov distance (KSD) between two distributions μ and ν is defined by

$$\text{KSD}(\mu, \nu) = \sup_{x \in \mathbb{R}^d} \|F_\mu(x) - F_\nu(x)\|, \quad (41)$$

where F_μ and F_ν denotes the cumulative distribution function of μ and ν respectively. We evaluate the 10-dimensional Funnel samples using the sliced version from [48, Appendix D.1].

Additional implementation details. For both targets, we use DSI to estimate the score. On Rings, we choose $R = 4, \tau = 0.15$ that satisfy Assumption 1 to initialize AIS, SMC, SMS, and SLIPS; and on Funnel, we use $R = 2.12, \tau = 0.0$, following the implementation of Grenioux et al. [9].

On Rings, we set the initial proposal distribution in Algorithm 3 for RDSMC and its variants to $\mathcal{N}(x_0 | x_t/\alpha_t, \sigma_t^2/\alpha_t^2)$. On Funnel, the above choice would render numerical instability when t is large. Hence we use $\mathcal{N}(x_0 | x_t, \sigma_t^2/\alpha_t^2)$ as the proposal for the AIS procedure.

Additional results. Additional results for the Rings experiment are provided in Table 5. We observe that RDSMC (Proposal) achieves the best overall sample quality, as measured by Sample W2, Radius TVD, and Angle TVD. While RDSMC’s Radius TVD closely matches the best performance, its Angle TVD and Sample W2 lag behind other baselines and RDSMC (Proposal). However, both RDSMC and its importance sampling (IS) variant achieve lower bias in estimating the log normalization constant compared to AIS and SMC.

D.4 Bayesian logistic regression

Targets. We consider four Bayesian logistic regression datasets: Credit and Cancer [35], Ionosphere [36] and Sonar [37].

- Credit [35]: this dataset addresses binary classification of individuals as good or bad credit risks. It contains 1000 data points with 25 standardized features.
- Cancer [35]: this dataset involves classifying recurrence events in breast cancer. It consists of 569 data points in a 31-dimensional standardized feature space.
- Ionosphere [36]: this dataset classifies radar signals passing through the ionosphere into good or bad categories. It features 351 data points with dimensionality $d = 35$.
- Sonar [37]: this dataset differentiates sonar signals reflected from metal cylinders versus cylindrical rocks. It includes 208 data points with $d = 61$ standardized features.

We consider a training dataset $\mathcal{D} = \{(x_j, y_j)\}_{j=1}^M$ where $x_j \in \mathbb{R}^d$ and $y_j \in \{0, 1\}$ for all $j \in \{1, \dots, M\}$. A Bayesian logistic regression model consists of the following

$$p(w, b) = \mathcal{N}(w; 0, \mathbf{I}_d) \mathcal{N}(b; 0, (2.5)^2) \quad (42)$$

$$p(y | x; w, b) = \text{Bernoulli}(y; \sigma(x^\top w + b)) \quad (43)$$

where $w \in \mathbb{R}^d$ is a weight vector, $b \in \mathbb{R}$ is an intercept, and σ is the sigmoid function.

The target distribution we are interested in is the posterior distribution

$$p(w, b | \mathcal{D}) \propto p(\mathcal{D} | w, b) p(w, b) = \prod_{j=1}^M p(y_j | x_j; w, b) p(w, b).$$

Metric. Following Grenioux et al. [9], we use the following definition of the predictive log-likelihood given a test dataset $\mathcal{D}_{\text{test}}$:

$$\frac{1}{N} \sum_{i=1}^N \sum_{(x,y) \in \mathcal{D}_{\text{test}}} \log p(w_i, b_i) + \log p(y | x; w_i, b_i) \quad (44)$$

where $\{w_i, b_i\}_{i=1}^N$ are posterior samples.

Additional implementation details. On all tasks, we use $R = 2.5, \tau = 0.0$ in Assumption 1 to initialize AIS, SMC, SMS, and SLIPS following the implementation of Grenioux et al. [9].

For RDSMC and its variants, we use TSI to estimate the score and clip the norm of the estimated score within 20 to improve numerical stability. We use $\mathcal{N}(x_0 | x_t/\alpha_t, \sigma_t^2/\alpha_t^2)$ as the initial proposal distribution in the AIS-based score estimation procedure.